

# **Dimensioneringsregler för brandutsatta lätta stålkonstruktioner**

Rapport till BRANDFORSK

Projekt 325-021  
Version 01

Stålbyggnadsinstitutet, SBI  
2004-09-27

## Sammanfattning

Intresset och stödet för utveckling av stålkonstruktioner i element- eller modulform till hus och byggnader har ökat i hela Europa. Lätta stålkonstruktioner har blivit alltmer populära som stomme i väggar och undertak samt som bärande stomelement utgörande delar av den bärande stommen i lagerbyggnader eller hus. I byggnader ställs ofta indirekta eller direkta brandtekniska krav på stålkonstruktioners brandmotstånd.

För närvarande finns det dock väldigt lite kunskap och inga funktionsdugliga regler för bedömning av lätta stålkonstruktioners (avskiljande byggelement) beteende vid brandpåverkan. För bärande konstruktioner är problemet mycket mer omfattande eftersom kallformat stål förekommer i väldigt många olika dimensioner och tvärsnittformer. Av denna anledning är det därför inte möjligt att tillämpa sig av dimensionering genom provning. Enda sättet är att utveckla dimensioneringsregler vid höga temperaturer som sedan kan inarbetas i Eurokoder och i standarder.

För att komma till rätta med ovan angivna problem initierade ECSC (European Coal and Steel Community) ett projekt, där syftet var att:

- öka förståelsen för det brandtekniska beteendet och brottmekanismen hos lätta stålkonstruktioner under brandpåverkan genom att utföra brandprovningar och numeriska simuleringar på provkroppar i liten skala och i full skala, inklusive några värmeflödesprov med naturliga brandförlopp,
- erhålla mer exakt data avseende de mekaniska egenskaperna hos kallformat stål vid höga temperaturer,
- kontrollera förmågan hos existerande datormodeller att simulera experimentella beteenden hos lätta stålkonstruktioner vid höga temperaturer,
- utveckla enkla beräkningsmodeller som beskriver beteendet hos brandutsatta lätta stålkonstruktioner, för användning vid brandteknisk dimensionering av bärande strukturer och extrapolering av provningsresultat för väggar och undertak med lätt stålstomme.

Stålbyggnadsinstitutet (SBI) har arbetat med att ta fram nya dimensioneringsregler för brandutsatta lätta stålkonstruktioner. SBI:s medverkan i projektet har i huvudsak inriktats på att analysera tunna kallformade profiler vid förhöjda temperaturer. Analyserna har utförts med FEM, kalibrerade mot verkliga brandförsök. FE-modellen har sedan använts som verktyg för att ta fram beräkningsmodeller för ostagade tunnplåtsreglar utsatta för brand. Beräkningsmodellen kan användas för att beräkna bär-förmågan för en ostagad tunnplåtsregel vid en viss temperatur med hänsyn till lokala och globala instabilitetsfenomen. Denna rapport är ett utdrag ur slutrapporten till RFCS projektet *Calculation rules for lightweight steel sections in fire situation* med projektnummer 7210-PR254 och beskriver det arbete som SBI i huvudsak har arbetat med.

För vidare information hänvisas till slutrapport, delrapporter och försöksresultat sammanställda på CD. Kontakta SBI eller BRANDFORSK för mer information. Projektet har finansierats av RFCS och BRANDFORSK. BRANDFORSK projektnummer är 325-021. En sammanfattning av hela projektet ges på följande sidor på engelska.

## General conclusions

During the last three and half years (from 1 July 2000 until the end of 2003), a research project, sponsored mainly by ECSC, the following partners have completed dealing with the fire performance of cold formed lightweight steel structures:

- CTICM (France - Coordinator of the project)
- CORUS (United Kingdom)
- CSM (Italy)
- LABEIN (Spain)
- ProfilArbed (Luxembourg)
- SBI (Sweden)
- VTT Building and Transport (Finland)

A detailed description in the final report provides all investigated technical features of the project, arranged to meet the following principal objectives:

- to increase understanding of the fire behaviour as well as failure mechanisms of lightweight steel structures under fire exposure by performing both fire resistance tests and numerical simulations on small and full scale specimens, including heating condition under natural fire developments;
- to obtain accurate data on the mechanical properties of cold formed steel at elevated temperatures;
- to check the ability of existing advanced calculation models to simulate the experimental behaviour of lightweight steel elements;
- to develop new simple calculation models on the fire behaviour of lightweight steel structures on the one hand for fire assessment of their load-bearing capacity, and on the other hand for extrapolating test results on small size lightweight steel partitions to real building partition walls of very large size.

In order to reach above aims, the project was divided into several tasks of which the leadership is shared between all involved partners. The main activity of each task as well as its outcome can be summarised as follows:

- **Material properties of cold formed lightweight steels at elevated temperatures**

As part of the fundamental data for mechanical resistance assessment, the material properties of cold formed lightweight steels were determined by conventional tests on three different steels at both room and elevated temperatures. The corresponding experimental results have been fully analysed and the strength reduction factors of studied steels have been derived. In order to incorporate, these results into future fire part of Eurocode, all corresponding reduction factors are given in such a way that they can be used directly in Eurocode mathematical model for describing stress-strain relationships of steel at elevated temperatures. In addition, the above results have been applied to the numerical modelling parts of this research for mechanical analysis of lightweight steel structures under fire situation. It has been clearly shown that in some cases, lightweight steel may have very poor behaviour at elevated temperatures if it is not made according to European standard and in

addition not applied to load bearing members. Therefore, attention must be paid in use of corresponding strength reduction factors.

- **Mechanical behaviour of cold formed lightweight steel members as well as their assemblies at room temperature**

Fire resistance assessment of structural members usually needs to be referred to room temperature performance. Consequently, a relative important part of the research work was focused on mechanical behaviour of cold formed lightweight steel members at room temperature. A full testing programme was carried out on the same types of studied elements under fire situation such as short stub columns, tall isolated studs, studs maintained by boards in various arrangements, floor and wall panels, as well as their assemblies. The experimental results were then compared to both design rules of part 1.3 of Eurocode 3 [1] and numerical modelling with advanced calculation models. This comparison shows that the design rules of part 1.3 of Eurocode 3 [1] give, in general, conservative load-bearing capacities of lightweight steel members and that advanced calculation models are capable of predicting their failure loads within acceptable limits and can be used in parametric studies.

- **Mechanical behaviour of lightweight steel members fully engulfed in fire**

As lightweight steel members are thin wall elements, they are very sensitive to local buckling behaviour. Therefore, it is important to know about the appropriate characteristic values to be used in fire design. Consequently, one part of the work of the project was focused on this aspect. The stub column tests have been carried out on three different C-type sections and one special section called as AWS. Then, the application of validated numerical modelling to different stub columns shows that under fire situation, not only the 0.2 % proof characteristic strength should be used to predict the local buckling resistance of lightweight steel members but also the current recommendation in part 1.2 of Eurocode [2] should be revised regarding lightweight steel. On the other hand, in some cases, lightweight steel members are used as load bearing elements without any fire protection and still need to provide certain level of fire resistance. In the project, this situation has been dealt with by means of both experimental and numerical approaches in which tall lightweight steel studs subjected mainly to compression were examined. These fire tests provide valuable information on overall instability failure at elevated temperatures of slender lightweight steel studs with C-type section. Based on relevant experimental results, numerical modelling has been performed to validate the capability of advanced numerical model to simulate the fire behaviour of this type of lightweight steel members. Finally, new simple calculation models (see paragraph 4.4) have been developed based on both results of parametric numerical studies on heated isolated lightweight steel members under compression and room temperature design rules of part 1.3 of Eurocode 3 [1]. These models can be applied manually to assess the fire resistance of lightweight steel members engulfed in fire.

- **Mechanical behaviour of lightweight steel members maintained by boards (as gypsum/calcium silicate boards or glazed panels), at elevated temperatures**

The majority of lightweight steel members are used together with boards to form floor, walls etc. In this case, they are generally maintained by these boards, which provide additional restraint to lightweight steel members leading to higher fire resistance. This common design situation is extensively investigated within this research project. Once again, both experimental and numerical approaches are used. A large number of fire tests have been carried out in which various parameters of maintained lightweight steel members, such as type of sections (dimension and section shape), loading conditions (eccentricity and applied load level), heating condition (standard and natural fire as well effect of internal insulation), nature of boards (standard and fire boards), maintained condition (one side or two sides maintained) were investigated in detail. In parallel, an important numerical modelling investigation was performed on both the thermal and mechanical behaviour of lightweight members associated with boards in which the validity of advanced calculation models was fully checked. Numerical parametric studies were carried out which allowed development of new simple calculation models (see paragraph 5.4) to assess the fire performance of lightweight steel members maintained by boards. This simple calculation model is on the same basis of that given for fully engulfed isolated lightweight steel members (see paragraph 4.4) so that they can be easily combined together for new proposals of future fire part of Eurocode 3.

- **Fire behaviour of load-bearing walls, floors and their assemblies**

This part of research work is dedicated to the global behaviour of lightweight steel frame systems, such as floor, wall and their assemblies. The work was focused mainly on experimental investigation in which several large scale of fire tests were carried out on both individual lightweight steel panel systems and assembled panel systems. These tests showed clearly that individual panels made of lightweight steel frames behaved in a very similar way to with the fully assembled panels. The junction between horizontal and vertical boards did not suffer from the deformation of floor or the wall. The panel failure modes, if they occurred in panels, were the same as the isolated tests. However, more attention must be paid to local squash failure of floor-wall joint, which apparently could occur with largely reduced concentrated load in fire situation. The performance of steel joists in floor panels was numerically studied and the good agreement with experimental results shows that advanced numerical models is fully convenient for prediction of lightweight steel members under pure bending.

- **Fire resistance assessment of high non load-bearing partition walls built with cold formed lightweight steel members and plasterboards**

There is a limit to the size of non load-bearing partition walls which can be tested with existed testing facilities. However, the size of real partition walls are often much greater than this limit (up to several times of tested size). Therefore, the last part of the research concentrated on development of a

simple extrapolation method of this special application case of lightweight steel structures. The proposed method is based only on some particular simple calculations for ease of application and is easily amenable to spreadsheet use (consisting of just one Excel page). It covers both mechanical resistance prediction of lightweight steel supporting members and deformation compatibility criteria of plasterboards so that the time to fall of plasterboards can be taken into account.

After a global review of the results obtained during this research project, it can be considered that the whole of the objectives initially predicted for this project have been satisfactorily reached. The behaviour of lightweight steel structures at elevated temperatures has been largely investigated not only by means of tests but also with advanced numerical models. Although all the features of lightweight steel members under fire situation were not covered because of the complexity of all possible cases encountered in real buildings with lightweight steel structures, simple calculation models have been developed for the most common types of application conditions of lightweight steel structures, which can be easily incorporated in future fire part of Eurocode for steel structures. Moreover, according to the outcome of this project, the following observations should be noted:

- In the fire part of Eurocode 3, a critical temperature of 350 °C is given as National Determined Parameter for steel members with class 4 cross sections. However, the results of this research have confirmed the findings of other experts for already several years that even very slender thin wall steel members could have a critical temperature exceeding easily 400 °C under quite high load level. Consequently, the critical temperature of 350 °C could lead to very conservative design and penalize consequently the use of steel. Therefore, it is so necessary to make available detailed design rules for fire assessment of thin wall steel members, not only for cold formed but also for hot rolled elements;
- Existing European design rules for steel members are based only on uniform heating condition related to steel elements fully engulfed in fire. However, if the steel cross section is exposed partially to fire, an important temperature gradient arises across the steel section. This kind of heating regime could significantly modify the fire performance of steel structural members, in particular when they are subjected to compression. In this case, steel members will be unsafely designed if average temperature in the cross section is used whereas they will be very conservatively assessed if the maximum temperature is adopted. Therefore, it is necessary to provide additional design rules for steel members under compression with varying temperature gradient.

## 4. MECHANICAL BEHAVIOUR OF INDEPENDENT LIGHTWEIGHT STEEL MEMBERS ENGULFED IN FIRE

### 4.1 GENERAL

The work reported in this chapter was focused on both experimental and numerical analysis of the mechanical behaviour of isolated lightweight steel members engulfed in fire. The experimental work was carried out by VTT and CTICM. In addition, the numerical simulations were performed by CTICM and SBI for the purpose of developing and validating a simple calculation model for this specific situation of lightweight steel members.

The experimental work comprised fire tests on five different lightweight steel sections to study the axial resistance capacity against local buckling of the short stub columns at elevated temperatures. These tests on short stub columns ( $L = 600$  mm or  $1000$  mm) were with centric loading kept constant during the test and with temperature increased nearly linearly as a function of time. For some sections fire tests were performed also on tall studs ( $L = 3500$  mm) to study global buckling behaviour of isolated lightweight steel members. The steel sections were of two different steel grades, S 350 GD + Z and S 280 GD + Z. The tests on short stub columns were performed at VTT and the tests on tall studs at CTICM.

Numerical analyses have been performed for both short stub column and tall stud tests with different computer codes. Once the numerical modelling validated against experimental results, the numerical parametric study has been made to check the validity of the simple calculation models and to develop design rules for isolated lightweight steel members under compression at elevated temperatures.

### 4.2 EXPERIMENTAL WORK

#### 4.2.1 Tests on short stub columns

##### 4.2.1.1 Testing methodology

Fire tests on the short stub columns were carried out in the model furnace ( $1.5 \times 1.5 \times 1.5$  m<sup>3</sup>) of the fire-testing laboratory of VTT, Espoo, Finland. Altogether nine tests were performed [31, 32].

Test specimens were short stub columns of five types of lightweight steel sections supplied by Corus (UK), Rautaruukki Oy (Finland) and Lafarge (France). The steel sections were of two different steel grades and the specimens were of two different lengths. Basic characteristics of the specimens are given in Table 4-1.

Section	Steel grade	Supplier	Length [mm]
<b>Small (C1); C 98-51/49-6/0.6</b>	280 MPa	Lafarge	600
<b>Medium (C2); C 150-57-13/1.2</b>	350 MPa	Corus	600
<b>Large (C3); C 250-80-21.5/2.5</b>	350 MPa	Rautaruukki Oy	1000
<b>AWS 150/1.2</b>	350 MPa	Rautaruukki Oy	1000
<b>TC 150/1.2</b>	350 MPa	Rautaruukki Oy	600

Table 4-1: Short stub column specimens

Section C1 was provided with service holes with a diameter of 31.8 mm and a spacing of 500 mm. The thickness of the zinc coating was 20  $\mu\text{m}$ , measured by VTT.

Section C2 was manufactured from pre-hot dipped galvanised steel to BS EN 10147 grade S350 GD + Z coating G274. The thickness of the coating was 22.5  $\mu\text{m}$ . The zinc coating in sections C3, AWS 150 and TC 150 is 275  $\text{g/m}^2$ , which corresponds to a thickness of 20  $\mu\text{m}$ .

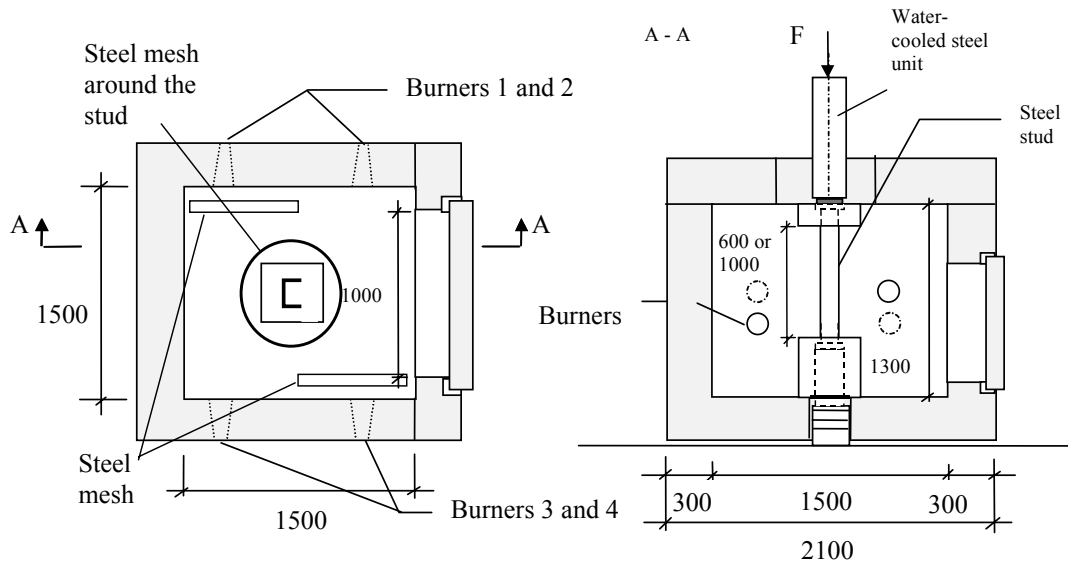
The influence of the service holes was also studied with section C2 that was tested both without a hole and with a hole ( $\varnothing$  35.2 mm) at mid-height of the specimen. Sections AWS 150 and TC 150 are perforated.

The specimens were tested with external centric load ( $N_{\text{Test,fi}}$ ) applied about 30 minutes before the starting of fire test and kept constant during the test. The load in tests 0 and 5 was applied by weights and in the other tests by a hydraulic jack controlled manually during the test. The test load was determined on the basis of the cross-sectional resistance of the sections determined at normal temperature ( $N_{\text{Test.ref}}$ ). The applied load levels were 0.07, 0.2, 0.4 and 0.6 for the C2 sections (Medium) and 0.4 for the others. Both ends of the specimens were free to rotate about strong axis but restrained to rotate about weak axis (see Figure 4-2).

At the beginning of the tests the furnace temperature reached 200°C in about 5 minutes and after that the heating rate was about 10°C/min. Perforated steel sheets surrounded the specimen to prevent the flames from the burners impinging the specimen and to ensure a uniform temperature distribution around the specimen. The diameter of the surrounding shield was about 500 mm.

During the fire tests the temperatures of the specimen were measured at three heights of the specimens. The furnace temperature was measured at the same levels with twelve thermocouples (K-type  $\varnothing$  3 mm stainless steel sheathed) on four sides of the specimen 100 mm from the surface of the specimen. The change of the length of the specimen was measured as vertical displacement of the top of the water-cooled steel unit above the specimen. The tests were conducted until the failure of the specimen.

The test programme is presented in Table 4-2. The test arrangement is presented in Figure 4-1 and 4-2, a photograph of a specimen in the furnace before fire testing in Figure 4-6 and the location of the measuring points in the C-sections in Figure 4-3. Photographs of the test specimens after the fire tests are shown in Figures 4-7 to 4-9.



Burners 1 and 4 were used in the tests.

Figure 4-1: Test arrangement in the furnace; horizontal and vertical sections.

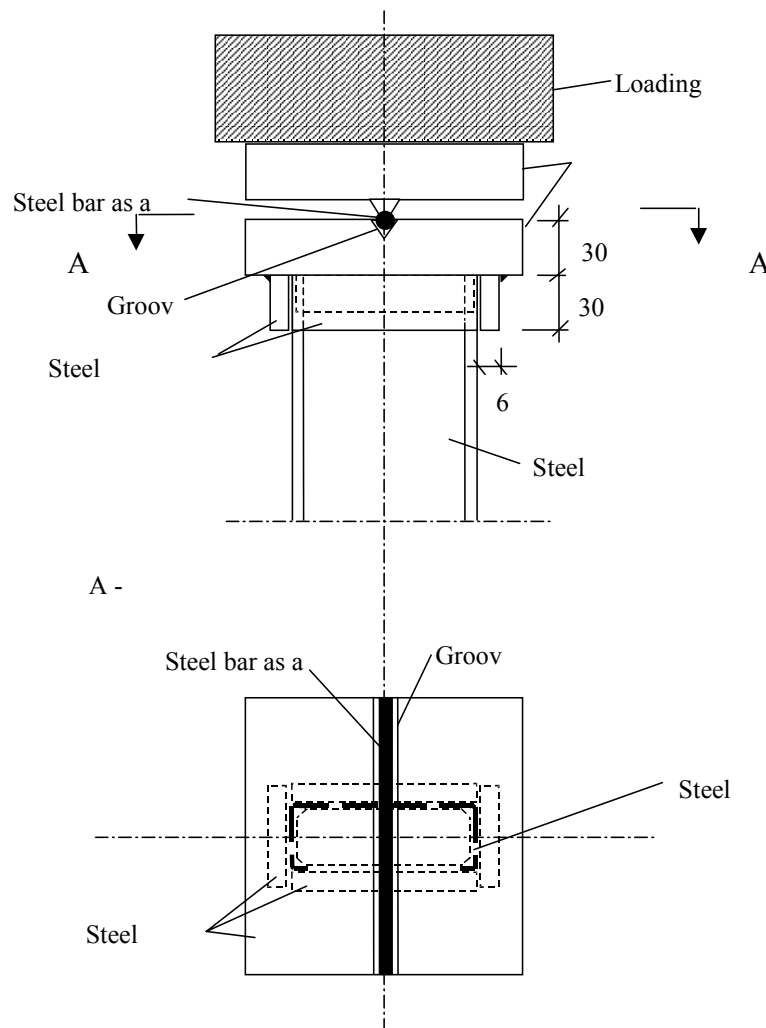


Figure 4-2: Support conditions of the steel stud.

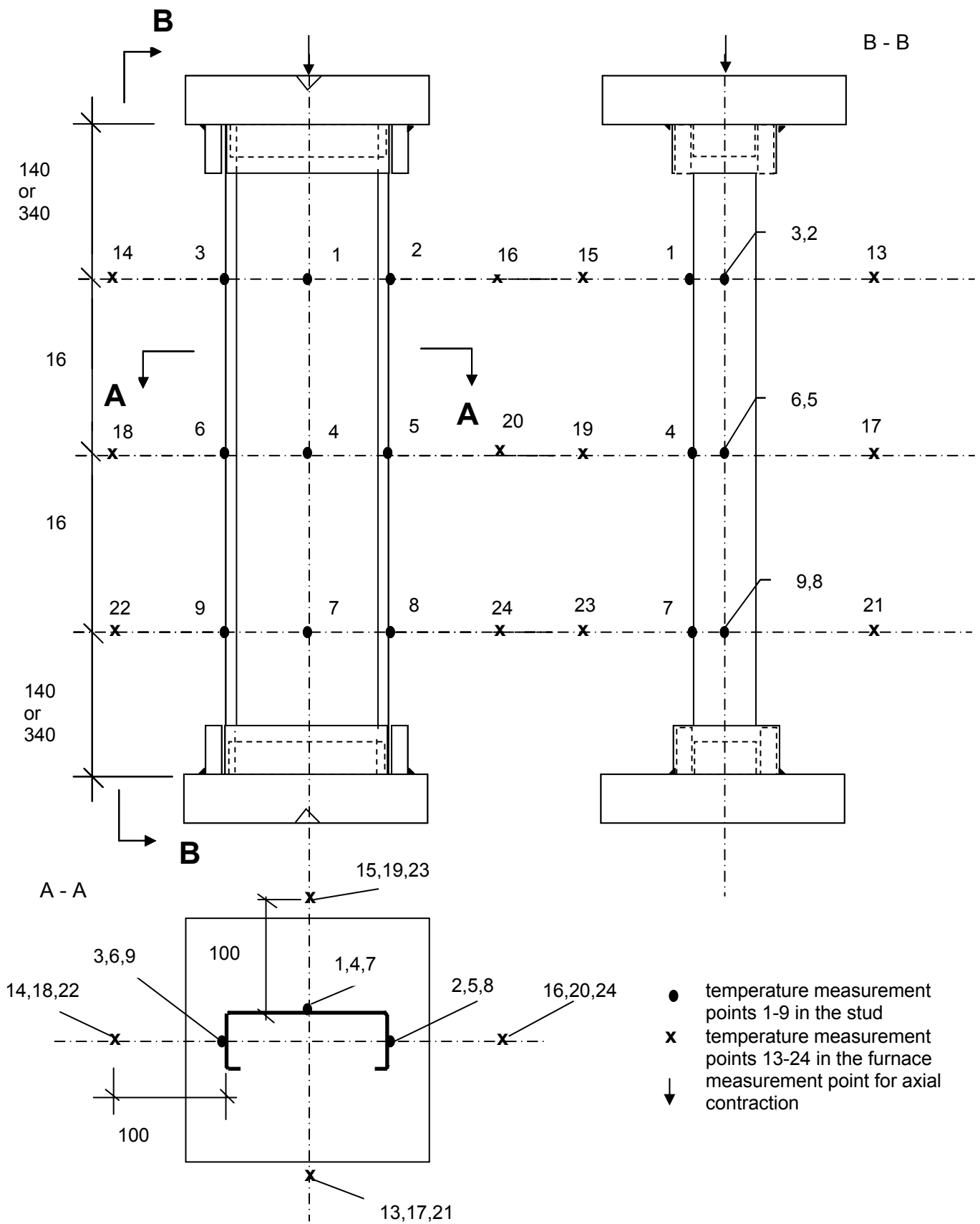


Figure 4-3: Position of the measuring points C-sections

### 4.2.1.2 Test results

The test results are summarized in Table 4-2. Test time (min) given in the table is the failure time of the specimen. The criteria for the failure time are the ability of the section to carry the test load. In the table also the temperature of the specimen at the failure time is given.

As an example, furnace and specimen temperatures measured at different levels in Test 3 are presented in Figures 4-4 and 4-5. Photographs of the specimens after the fire tests are in Figures 4-6 to 4-9.

Fire test	Stud	Length (mm)	$N_{\text{Test.ref.}}$ (kN)	$N_{\text{Test.fi}}$ (load level) (kN)	Max temperature of failure (°C)	Test time (min)
<b>Test 0</b> 20.2.2002	C 150-57-13/1.2	600	59.6	3.9 (0.07)	1082	94.4
<b>Test 1</b> 25.2.2002	C 150-57-13/1.2	600	59.6	35.8 (0.6)	408	26.7
<b>Test 2</b> 27.2.2002	C 150-57-13/1.2	600	59.6	11.9 (0.2)	680	53.0
<b>Test 3</b> 1.3.2002	C 150-57-13/1.2	600	59.6	23.8 (0.4)	531	39.0
<b>Test 4</b> 5.3.2002	C 150-57-13/1.2 with service hole	600	67.4	23.8 (0.4)	534	37.8
<b>Test 5</b> 7.3.2002	C 100-50-6/0.6	600	8.6	3.3 (0.4)	491	32.8
<b>Test 6</b> 19.3.2002	AWS 150/1.2	1000	74.1	29.6 (0.4)	638	47.0
<b>Test 7</b> 22.3.2002	C 250-80-22/2.5	1000	195.5	78.2 (0.4)	618	43.7
<b>Test 8</b> 7.3.2003	TC 150-1.2	600	41.5	16.6 (0.4)	630	48.0

Table 4-2: The results of short stub column tests performed at room temperature and at elevated temperatures

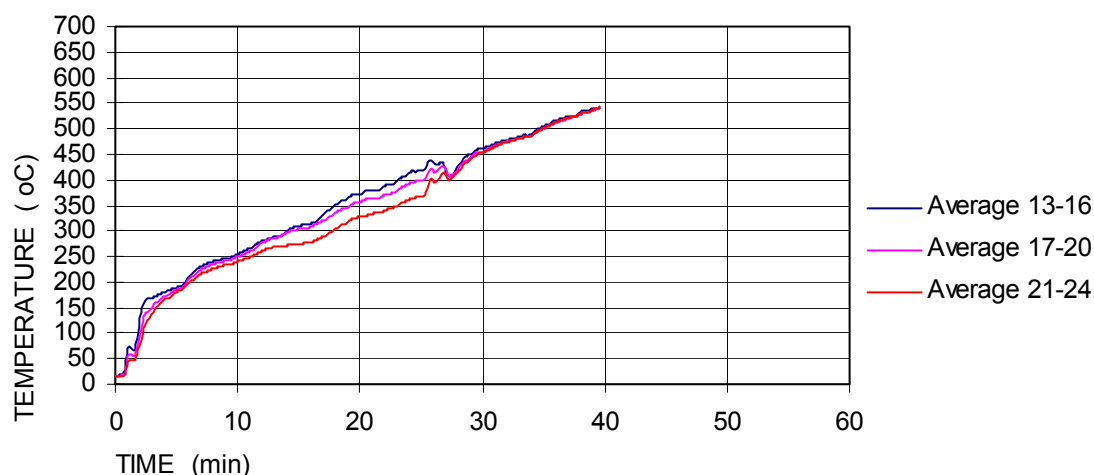


Figure 4-4: Average temperature of the furnace in Test 3

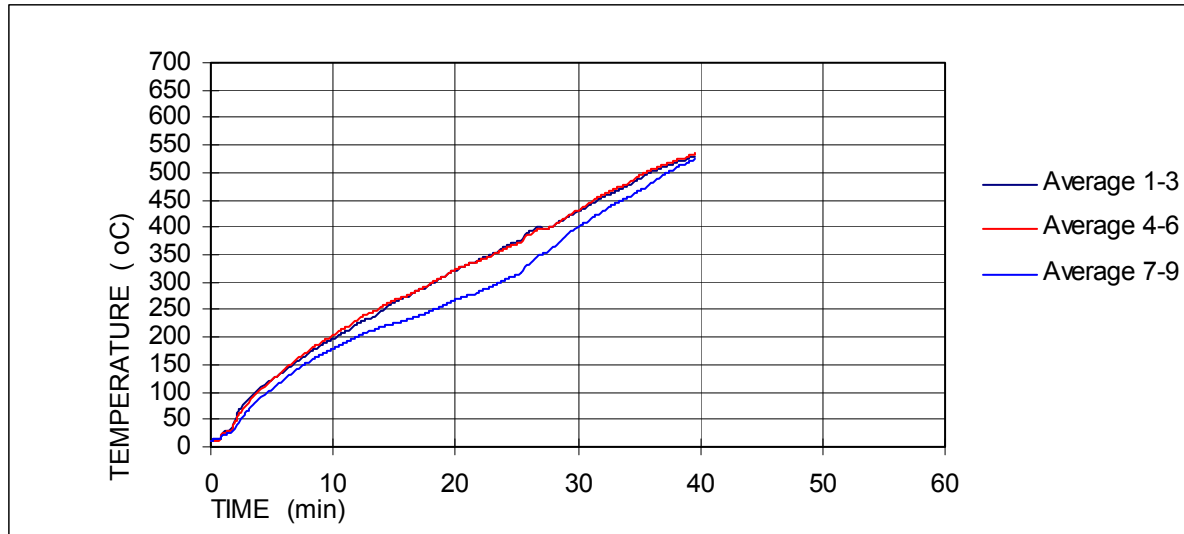


Figure 4-5: Specimen temperatures at different levels in Test 3



Figure 4-6: Mounting of the specimen (AWS-section)



Figure 4-7: Test specimens 1–4 after the fire tests



Figure 4-8: Test specimens 4–7 after the fire tests



Figure 4-9: Test specimen 8 after fire test

#### 4.2.1.3 Summary of test results

The axial resistance of five cold-formed lightweight steel sections (C 100, C2 150, C3 250, AWS 150 and TC 150) was determined with tests on short stub columns ( $L = 600$  mm or  $1000$  mm) both at room and at elevated temperatures.

The fire tests were performed with different load levels. The load level for section C 150 were 0.07, 0.2, 0.4 and 0.6 and for the others 0.4. The cross sectional resistance  $N_{\text{Test,ref}}$  determined at room temperature was used to set the test loads in fire tests.

The dependence of the failure temperature on the load level ( $N_{\text{Test,fi}}/N_{\text{Test,ref}}$ ) is shown in Figure 4-10. Load level 1 corresponds the axial resistance at ambient temperature ( $N_{\text{Test,ref}}$ ). Load level being 0.4 the failure temperatures were  $491$  °C for section C 100,  $534$  °C and  $531$  °C for sections C2 150 (one without a hole and one with a hole),  $618$  °C for section C3 250 and  $638$  °C for AWS 150 section and  $630$  °C for TC 150 section. The dependence of the strain on the steel temperature is shown in Figure 4-11.

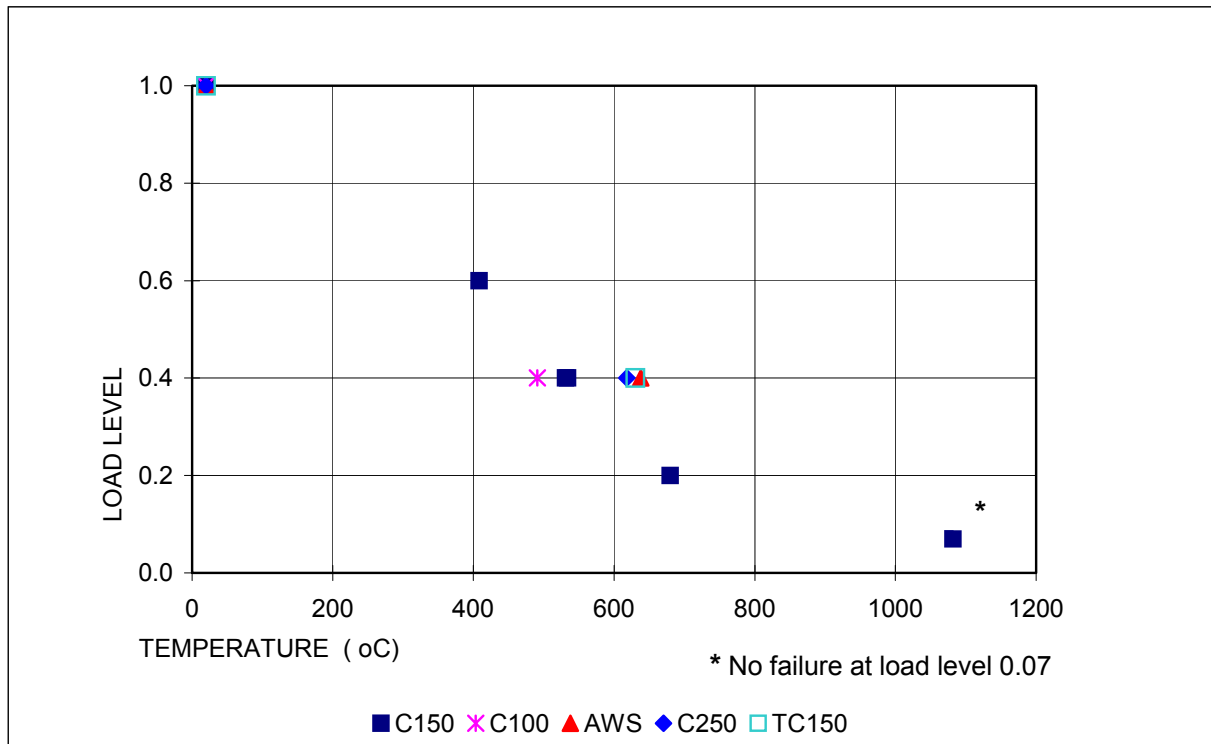


Figure 4-10: Failure load level ( $N_{Test.fi} / N_{Test.ref}$ ) as a function of the temperature for different steel sections (Load level 1.0 corresponds to reference load  $N_{test.ref}$ )

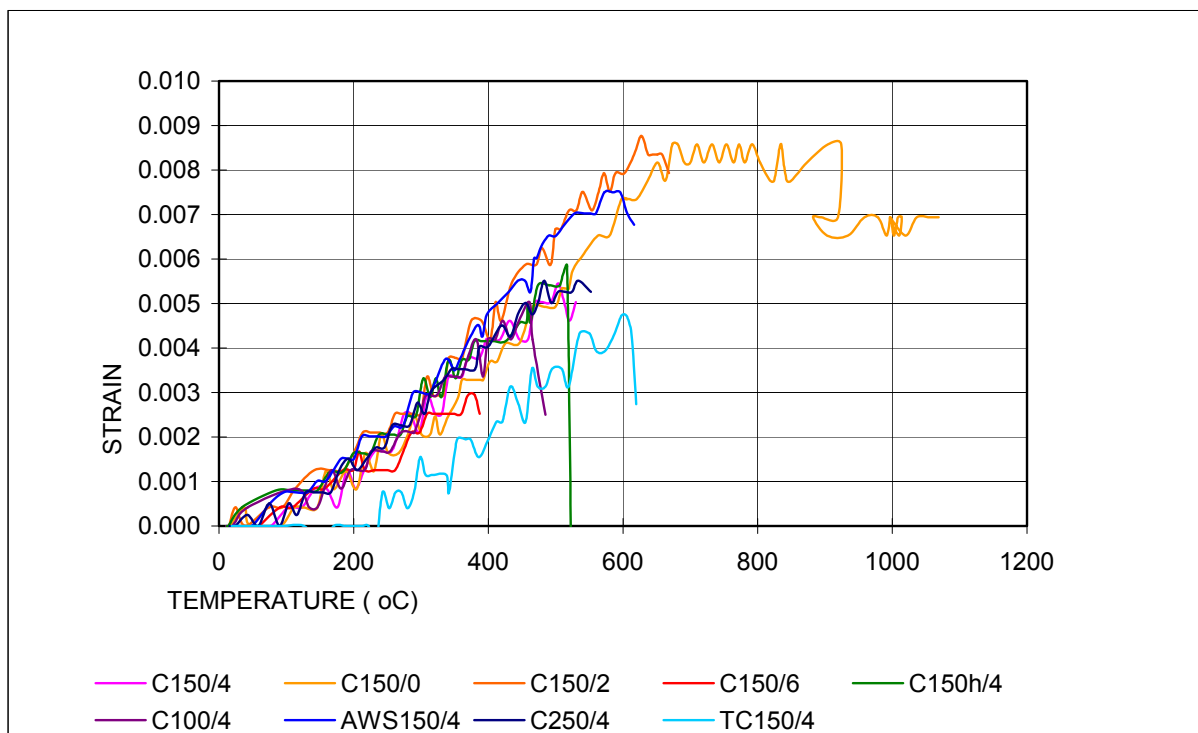


Figure 4-11: Strain ( $\Delta L/L$ ) as a function of temperature for different steel sections and load levels

## 4.2.2 Test on tall studs

### 4.2.2.1 Testing methodology

Fire tests on tall studs fully engulfed in fire were performed at CTICM. Altogether six tests were performed.

The specimens were 3500 mm tall steel studs of three different types of lightweight steel sections designated as Medium, Large and AWS. The basic characteristics of the steel sections are given in paragraph 4.2.1.1.

In the fire tests, all specimens were subjected to an axial load, which were applied before the test and kept constant until failure. Some specimens were tested with eccentric load. At room temperature, the specimens were considered as hinged at one end and restrained against rotation at the other end about the strong axis. All rotations about weak axis at both ends of studs are assumed to be restrained. The boundary condition in AWS section stud test is presented in Figure 4-12.

During all the tests, the furnace temperature was continuously recorded. In order to determine the temperature field in the steel studs, thermocouples were installed on the steel studs (both flanges and web) at four different levels N1, N2, N3 and N4 along the specimen length. The positions of thermocouples are shown in Figure 4-13 for the C-sections and in Figure 4-14 for the AWS section.

Lateral and longitudinal displacements of the specimens were recorded during the tests. The location of the displacement measurements for the AWS section is presented in Figure 4-15.

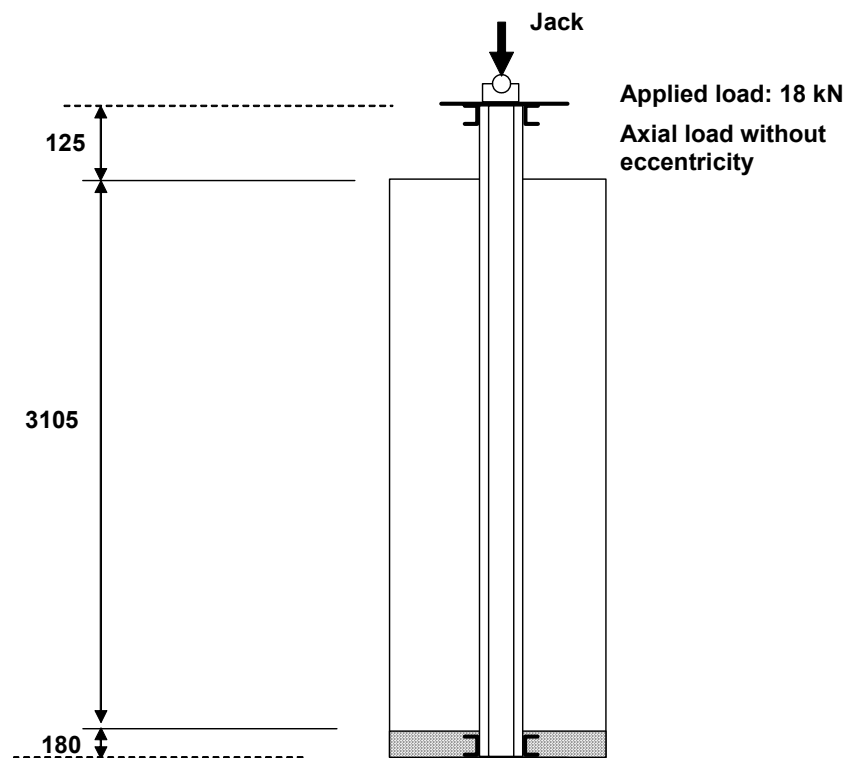


Figure 4-12: Boundary condition of AWS section stud test

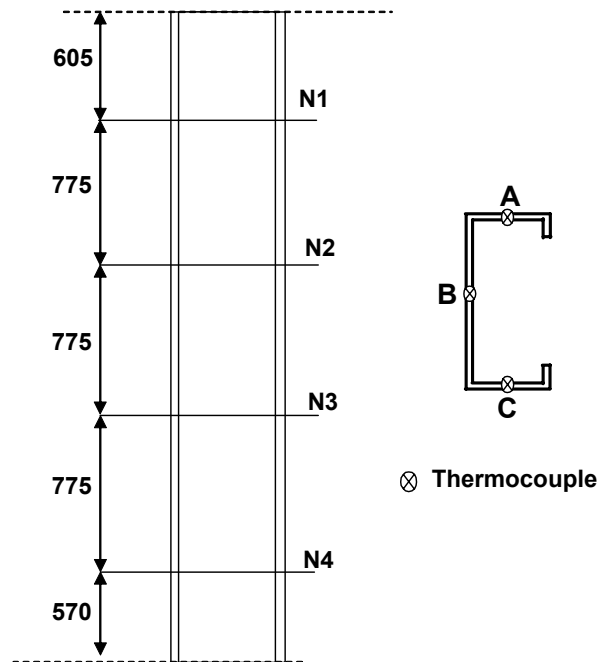


Figure 4-13: Location of the temperature measurement points in the C-sections

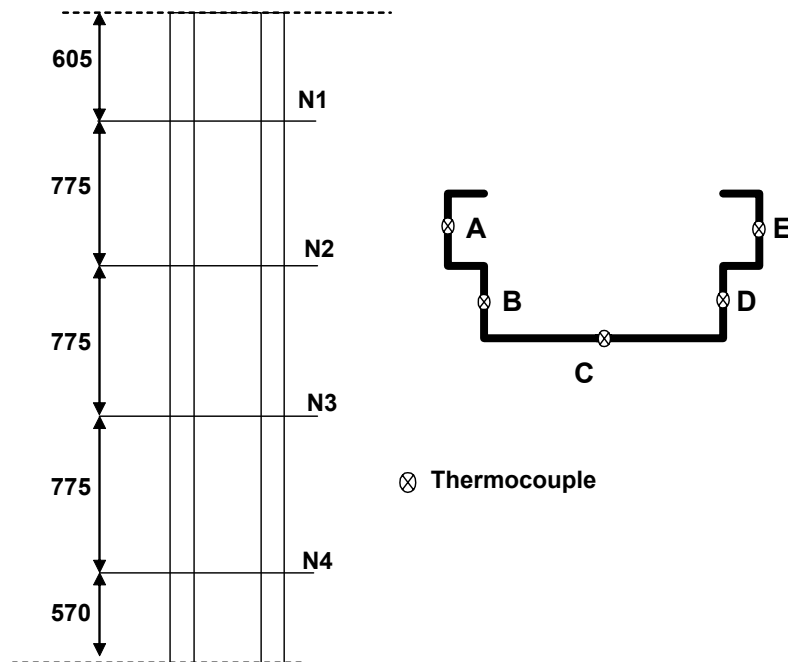


Figure 4-14: Location of the temperature measurement points AWS section

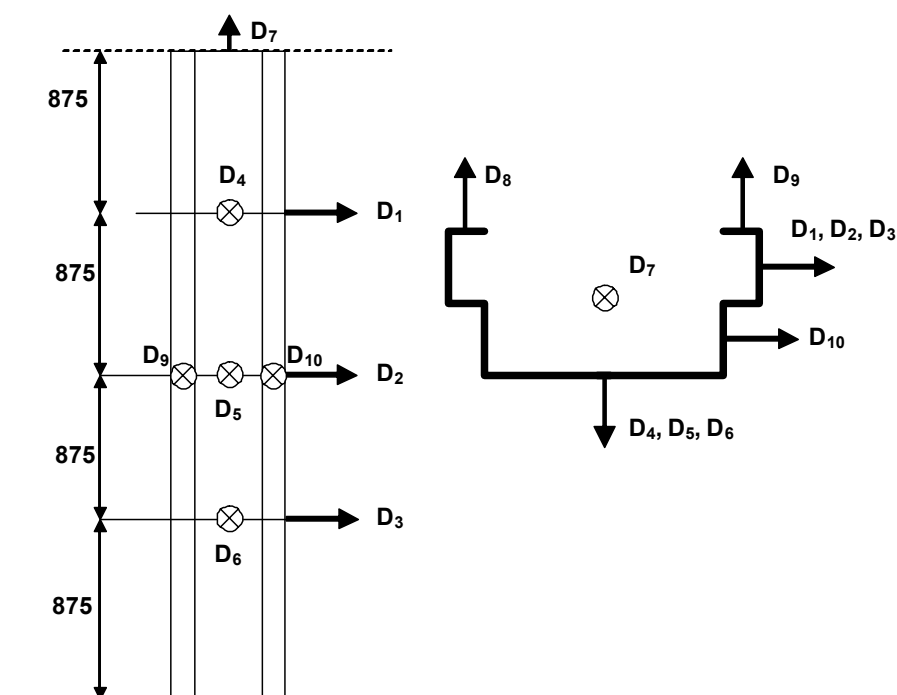


Figure 4-15: Location of the displacement measurement points in AWS section

The test program is presented in Table 4-3.

#### 4.2.2.2 Test results

The failure time measured during the tests, which are reported in Table 4-3, corresponds to the condition when each specimen (steel stud) could not carry the applied load any more.

Test	Stud	Length (mm)	Loading condition		Maximum Temp. (°C)	Test time (min)
			Load (kN)	Ecc. (mm)		
03-S-373	medium	3500	15	37.5	257.0	18.0
03-S-357	medium	3500	25	0	245.0	23.0
03-S-369	medium	3500	15	0	500.0	28.5
03-S-316	large	3500	60	0	565.0	57.0
03-S-348	large	3500	60	0	540.0	51.0
03-S-379	AWS	3500	18	0	529.0	35.0

Table 4-3: Summary of fire tests on tall studs

As an example, temperatures measured at different levels in the test on the AWS section are presented in Figures 4-16 to 4-19, lateral displacements measured along strong axis and along weak axis of AWS section in Figures 4-20 and 4-21 and vertical displacement in Figure 4-22. The actual applied load during the test is presented in Figure 4-23.

Some specimens after the tests are shown in Figures 4-24 to 4-26 in order to give an idea about the failure mode of these studs.

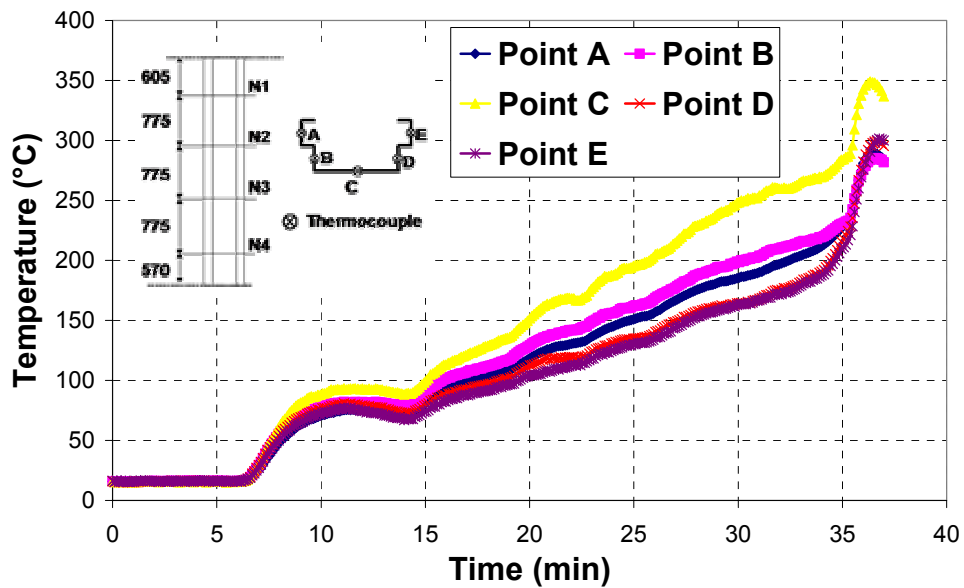


Figure 4-16: Temperatures measured on section N1 versus time in the test on AWS section

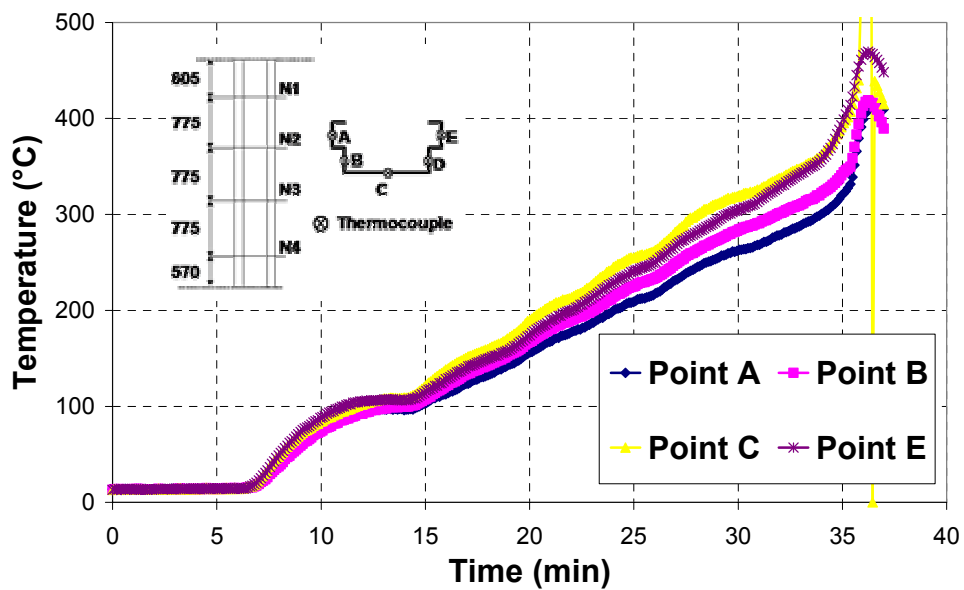


Figure 4-17: Temperatures measured on section N2 versus time in the test on AWS section

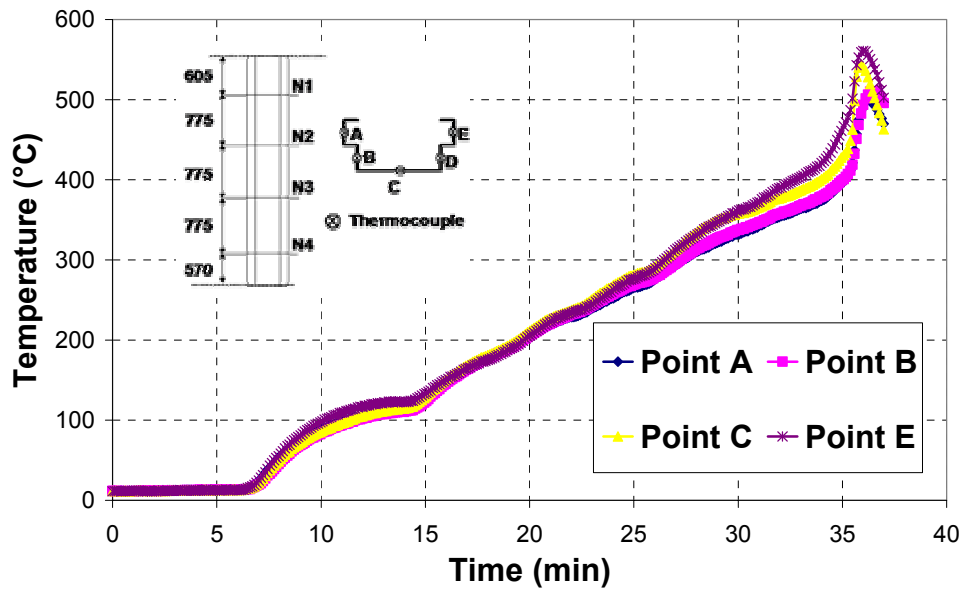


Figure 4-18: Temperatures measured on section N3 versus time in the test on AWS section

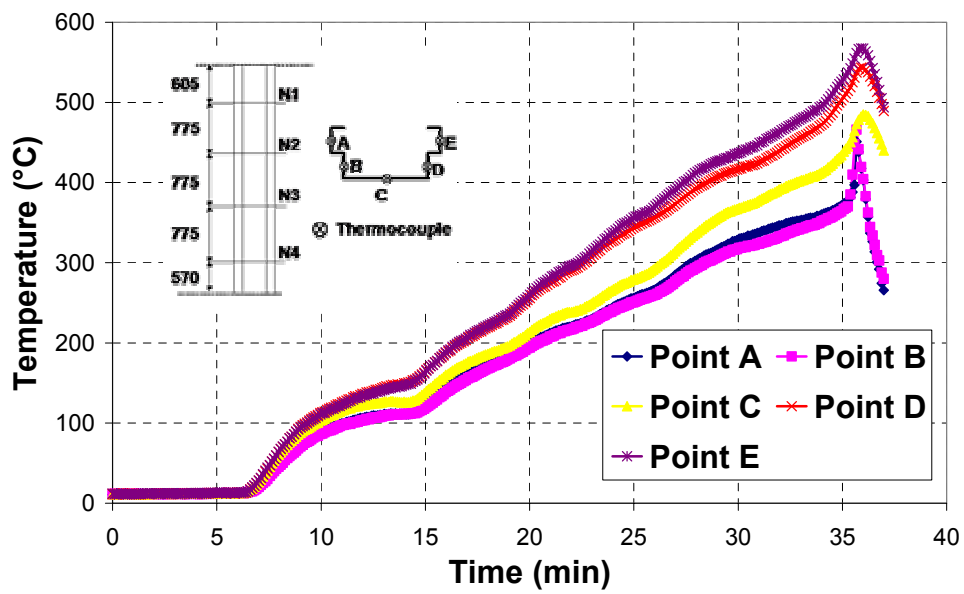


Figure 4-19: Temperatures measured on section N4 versus time in the test on AWS section

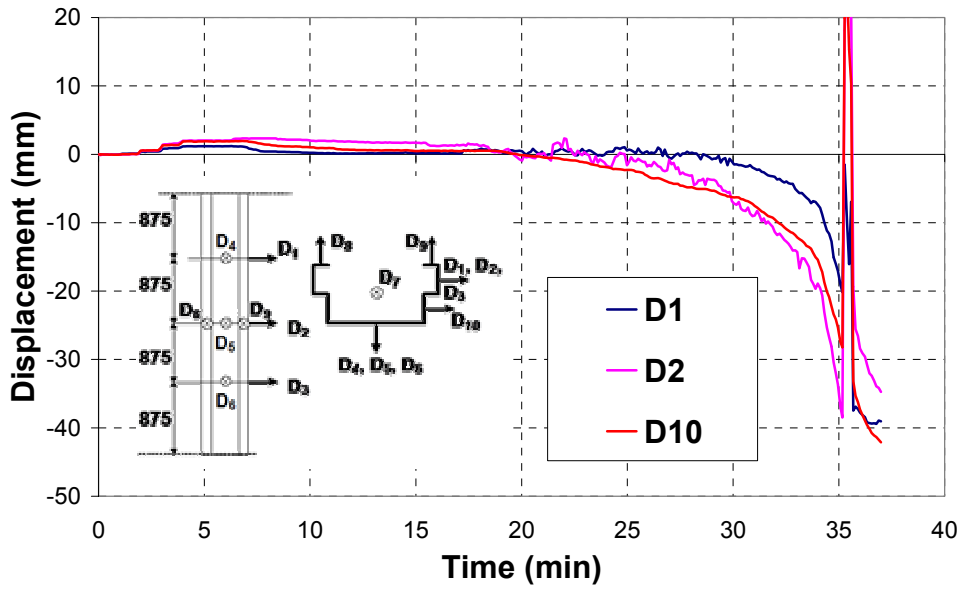


Figure 4-20: Lateral displacements measured along strong axis versus time in the test on AWS section

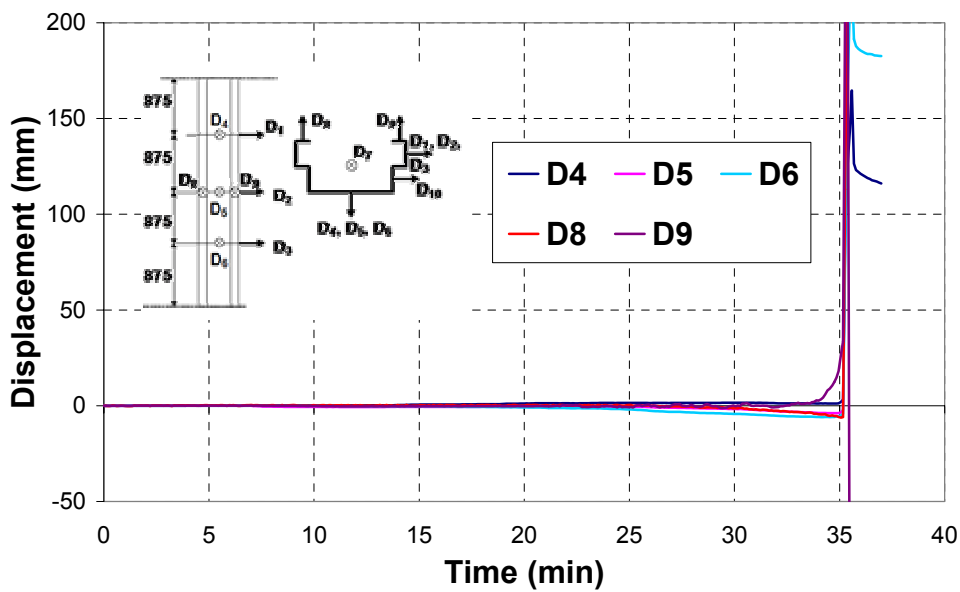


Figure 4-21: Lateral displacements measured along weak axis versus time in the test on AWS section

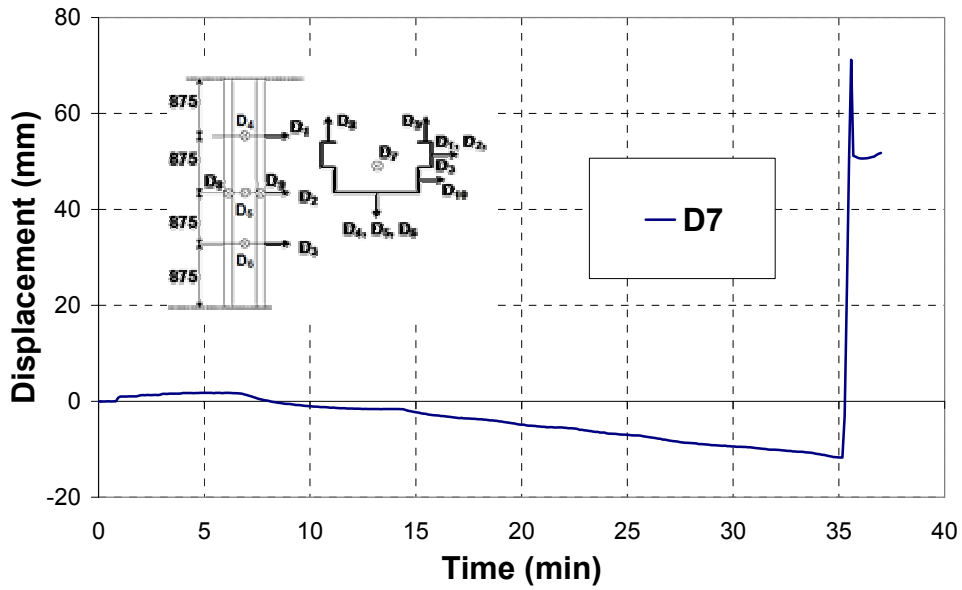


Figure 4-22: Measured vertical displacement versus time in the test on AWS section

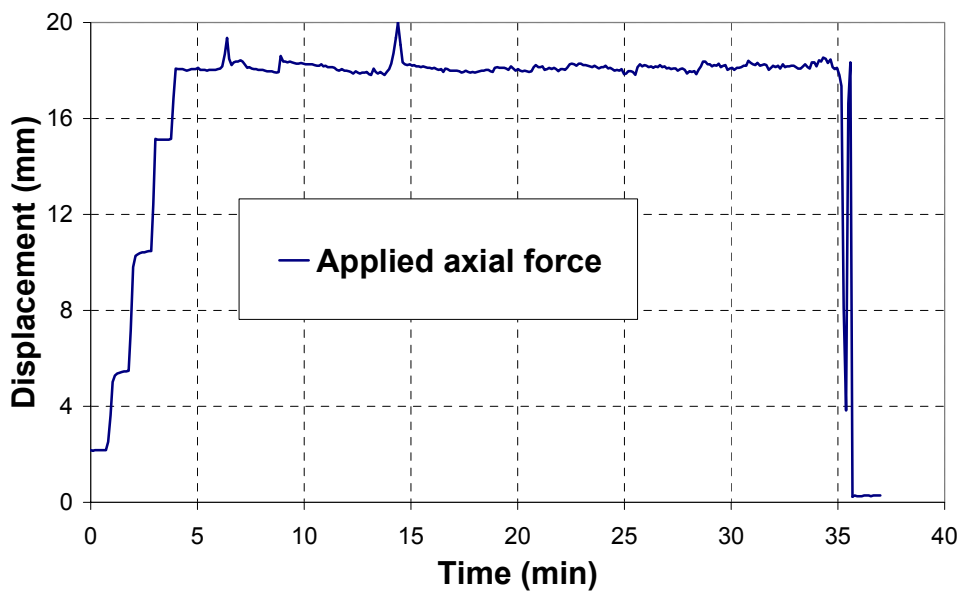


Figure 4-23: Measured applied force versus time in the test on AWS section



Figure 4-24: C-sections specimens after the fire tests (C 250)



Figure 4-25: C-sections specimens after the fire tests (C 250)



Figure 4-26: AWS-section specimen after the fire test

#### 4.2.2.3 Comparison between the results of tests on short and tall columns

The failure temperatures of the steel sections C 150, C 250 and AWS 150 in function of the load level in the tests on short (600 mm and 1000 mm) and tall (3500 mm) columns are presented in Figure 4.27. For C 150 section the failure temperature of the tall columns is

100-200 °C lower than that of the short columns with load levels 0.2 - 0.6. For C250 and AWS 150 sections the corresponding difference is about 100 °C with a load level of about 0.4,

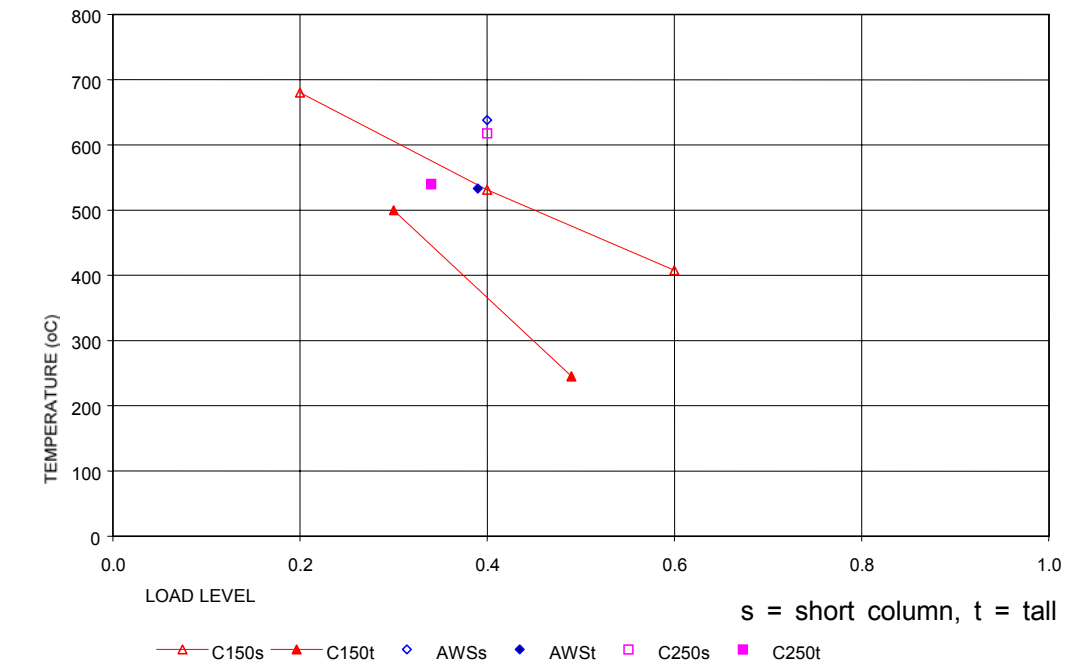


Figure 4-27: Failure temperatures of different steel sections in function of load level in fire tests on short short and tall columns

## 4.3 NUMERICAL SIMULATIONS OF FIRE TESTS

### 4.3.1 General

Numerical studies of the mechanical behaviour of isolated lightweight steel sections engulfed in fire were performed by both SBI and CTICM. The numerical simulations have been made based on the fire tests carried out at CTICM and VTT to validate the calculation model. Tests were performed on short (600 or 1000 mm) stub columns and tall (3500 mm) studs under constant load during the fire test. Also numerical simulations at room temperatures were made in order to validate numerical model.

One of the purposes of the simulations was to validate the proposed reduction factors for steel at elevated temperatures agreed in Chapter 2. The tests made on stub columns (600 or 1000 mm) at VTT at both room and elevated temperatures were used to verify the validity of these reduction factors through numerical simulations.

This paragraph also gives a proposal of a simple calculation method based on parametric studies of isolated steel studs engulfed in fire with and without temperature gradient.

## 4.3.2 Numerical modelling of stub column tests

### 4.3.2.1 Description of numerical modelling

Four different types of steel sections have been evaluated which are referred here as small, medium, large and AWS sections. The types as well as the dimensions of these sections have already been illustrated in detail in previous paragraphs.

The geometric data used in the numerical modelling of elevated temperature tests is from both measured values on test specimens and also nominal values. The web-heights, flange-widths and the edge stiffeners length are taken as nominal values. The thickness of the profiles and the radius of the rounded corners are taken as the measured values. All these values are indicated respectively in Tables 4-4 and 4-5.

In all stub column tests the load was applied centric to the steel section as shown in Figure 4-3.

Element	Small section	Medium section	Large section	AWS section
Length (l)	600	600	1000	1000
Web height (h)	100	150	250	20 + 110 + 20
Flange width (b)	50	57	80	40 + 50
Edge stiffener length (c)	6	13	21.5	15.5
Inner radius (r)	1.8	1.2	4.5	3.2
Thickness (t)	0.6	1.2	2.5	1.2

Table 4-4: Geometric data for the tested stub columns - nominal values (mm)

Element	Small section	Medium section	Large section	AWS section
Inner radius (r)	2.25	6	4.5	3.5
Core thickness ( $t_{core}$ )	0.56	1.155	2.41	1.145

Table 4-5: Measured geometric data for core thickness and corner radius used in the numerical calculations (mm)

The details of numerical modelling have been fully explained in paragraph 3.5.1. The material model used at elevated temperatures in the numerical calculations are based on the material model given in part 1-2 of Eurocode 3 [2], also explained in paragraph 2.6.2, with the yield strength and ultimate tensile strength presented in Table 2-2c, based on tensile tests performed by VTT for the tested specimens. The reduction factors used in the material model were taken as the proposed values from paragraph 2.6.3 (see Table 2-9 for **Type A** steel from small section and Table 2-10 for **Type B** steel from medium, large as well as AWS section). Conversely, in order to fully characterise the material model at room temperature, the stress-strain relationship for each investigated steels was taken as the tensile test results at room temperature explained in paragraph 2.4.1.

In order to investigate the validity of the reduction factors derived from tests, they are directly included into the material model to simulate the material behaviour at elevated temperatures of the specimens.

The thermal elongation was taken as the temperature dependent coefficient given in part 1-2 of Eurocode 3 [2] (see also Figure 2-12).

#### 4.3.2.2 Numerical results

The stub column tests of C-type cross section at elevated temperatures made by VTT was analysed with computer code ABAQUS. The temperature evolution in the steel stud was measured during the tests at several points as shown in Figure 4-28. The temperatures used in the numerical modelling were taken as the average value along and also across the section. One example is shown in Figure 4-28 for the medium section. Since the thermocouples in the tests stop recording the temperature evolution in the steel stud when the experiment stops the temperature evolution must be extended in order to simulate the extension of the temperature curve. This was done in the numerical modelling by extrapolation of the temperature curve from the tests.

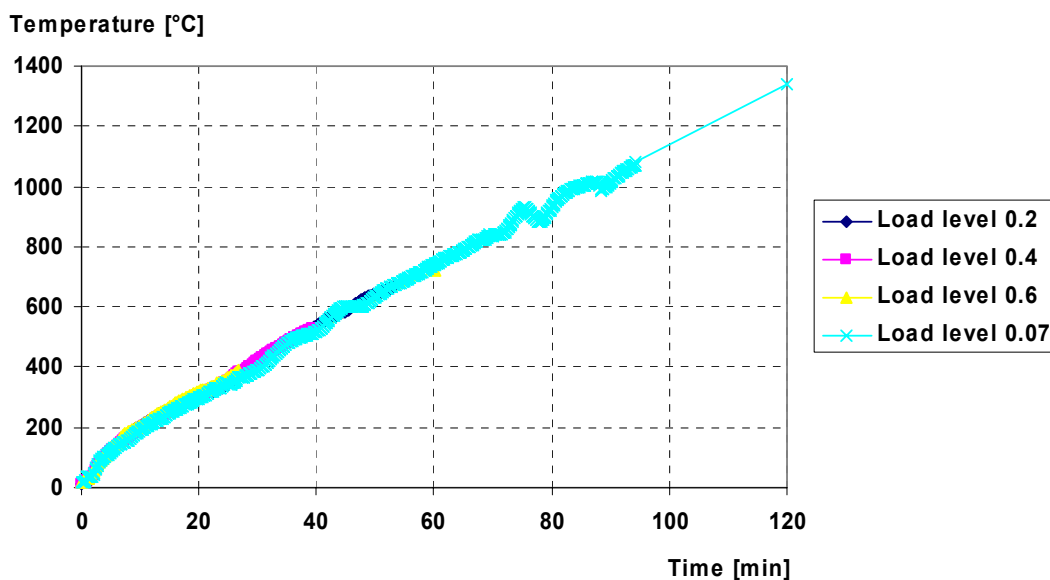


Figure 4-28: Temperature evolution in numerical modelling for medium section with load levels 0.07, 0.02, 0.4 and 0.6

The results are shown in Figure 4-29. As seen from the comparison between numerical calculations and test results, the agreement is fully satisfactory since the relative difference of critical temperature is within 10% for all sections.

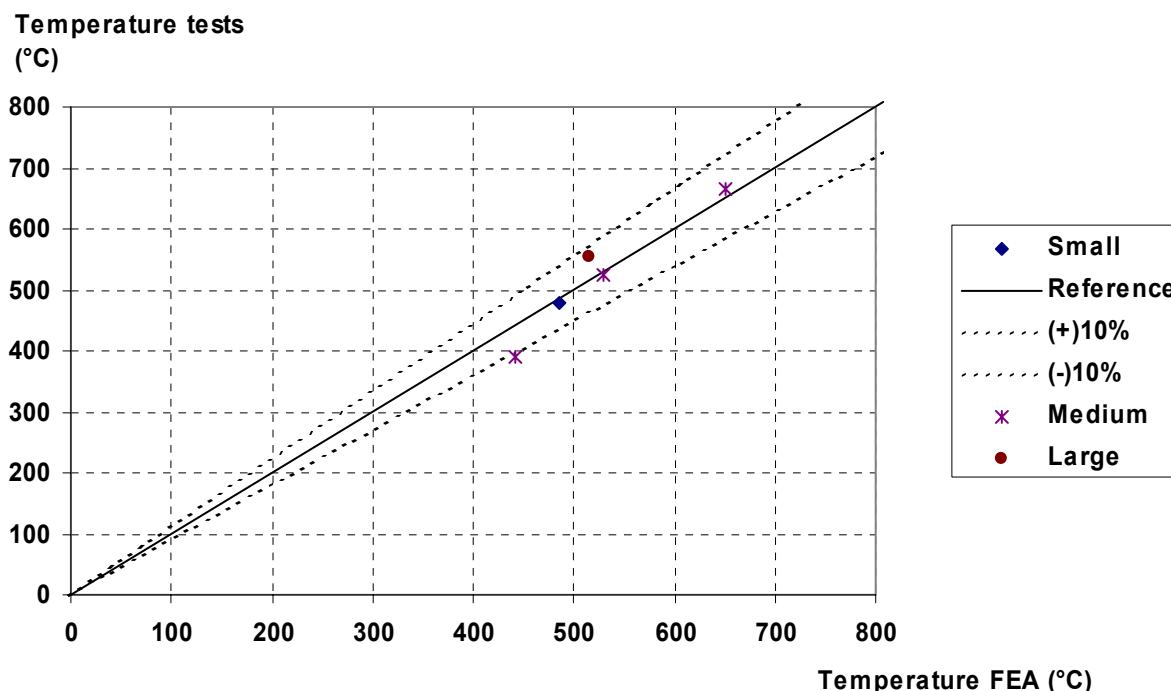


Figure 4-29: Comparison of failure temperatures for the different tested steel studs with numerical calculations

#### 4.3.2.3 Evaluation of proposed reduction factors

A parametric study was performed to investigate the proposed reduction factors for **Type A** steel and **Type B** steel, also explained in Chapter 2. In fact, this study can give an idea about the value to be used to calculate the design buckling resistance at elevated temperatures for lightweight steel members.

A comparison was made between different reduction factors given in part 1-2 of Eurocode 3 [2] and within this report. The numerical calculations were made with the proposed material model explained in Chapter 2. The ultimate resistance equivalent to corresponding temperature is normalised to room temperature resistance. In this way the appropriate reduction factor for simple calculation was evaluated. The failure of the steel stud depends on local buckling, which means that  $N_u = A_{eff} f_y$ . The results (see Tables 4-6 and 4-7) show that there is a good agreement by using the 0.2% proof strength for **Type A** steel and **Type B** steel respectively to calculate compression resistance considering local buckling. However, it can be seen that the reduction factor for 0.2% proof strength given in part 1-2 of Eurocode 3 is systematically higher, in particular for small section (**Type A** steel). Considering the good agreement between proposed reduction factors in this project and test results, it is therefore necessary to modify actual values of Eurocode. Nevertheless, as **Type A** steel investigated within the project is used only in case of non loadbearing partition walls and in addition its origin as well as its quality is not known, the modification to Eurocode values must not be based on the results of this steel (**Type A** steel) but should refer to the results of **Type B** steel.

Temperature	2.0 % - Chapter 2	0.2 % - Chapter 2	2.0 % - EC3	0.2 % - EC3	Numerical calculation (Small section)
20	1.000	1.000	1.000	1.00	1.00
200	1.000	0.849	1.000	0.89	0.88
400	0.560	0.310	1.000	0.65	0.35
600	0.200	0.110	0.470	0.30	0.13
800	0.060	0.042	0.110	0.07	0.05
1000	0.027	0.023	0.040	0.03	0.03

Table 4-6: Comparison between different reduction factors and numerical calculations on small section (**Type A** steel)

Temperature	2.0 % - Chapter 2	0.2 % - Chapter 2	2.0 % - EC3	0.2 % - EC3	Numerical calculation (Medium section)	Numerical calculation (Large section)
20	1.000	1.000	1.000	1.00	1.00	1.00
200	1.000	0.896	1.000	0.89	0.88	0.85
400	0.890	0.616	1.000	0.65	0.57	0.54
600	0.340	0.229	0.470	0.30	0.21	0.20
800	0.070	0.049	0.110	0.07	0.05	0.05
1000	0.0035	0.025	0.040	0.03	0.03	0.02

Table 4-7: Comparison between different reduction factors and numerical calculations on medium and large sections (**Type B** steel)

### 4.3.3 Numerical modelling of high studs engulfed in fire

#### 4.3.3.1 Elevated temperature simulations with C-type section tall studs

The numerical simulations of the mechanical behaviour of unbraced steel studs engulfed in fire were made with the computer code ANSYS. The following assumptions were used:

- The whole steel stud is modelled with shell element (see Figure 4-30)
- Steel studs are hinged at both ends about strong axis of the stud and subjected to a constant load during the fire (figure 4-30). Moreover, both ends of steel stud are modelled using a stiffer material (corresponding to blue colour element) with the value of modulus of elasticity taken as  $210 \times 10^5$  MPa

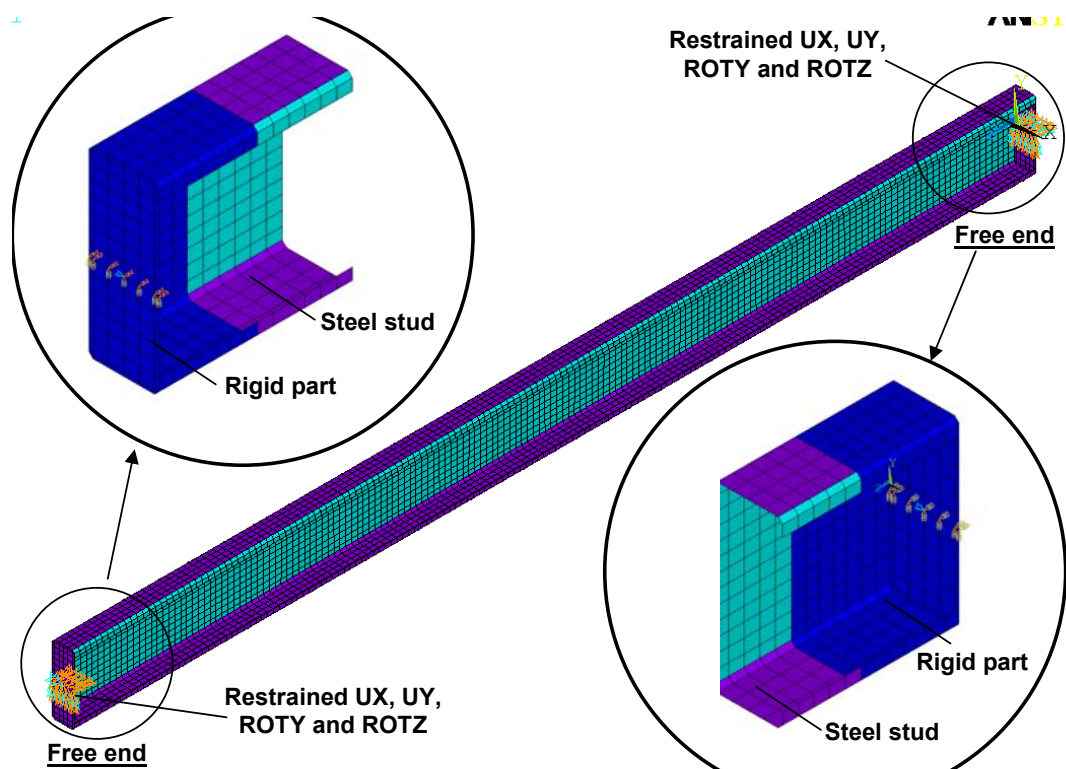


Figure 4-30: Example of boundary conditions adopted for steel studs

- Initial imperfection obtained from eigenvalue buckling analysis is used in numerical simulations. It consists of sinusoidal waves in the web with maximum amplitude of 1 mm.
- The mechanical materials properties have been taken to be in accordance with the proposed reduction factor for steel of both non load and load bearing members (see Chapter 2), with the mechanical properties at room temperature given in Table 2-2b
- The axial load is applied as a surface load as shown in figure 3-37. The load application direction (parallel to length of the stud) is kept constant whatever the stud end rotation is
- A temperature gradient along the length of the steel studs shown in Figure 5-31 is taken into account, which is based on temperature measurement from 4 sections N1, N2, N3 and N4 with a linear variation of temperatures between two successive sections and a uniform temperature distribution between N1, N2 and their corresponding stud ends
- Concerning the temperature distribution on cross section, the temperature is constant in each of two flanges, and varies linearly from one flange to the centre of the web, then linearly again from the centre of the web to the other flange (see figure 5-32).

The numerical simulations have been performed on 5 fire tests carried out at CTICM. One example of these calculations is given in figure 4-31 and the results of all calculations are summarised in Table 4-8, in which the critical temperature calculated for each specimen is compared with the experimental maximum temperature at failure time. It can be found that the agreement between calculation and test is generally very satisfactory except one test which can be explained by the fact that the real temperature gradient could be different from that used in numerical modelling.

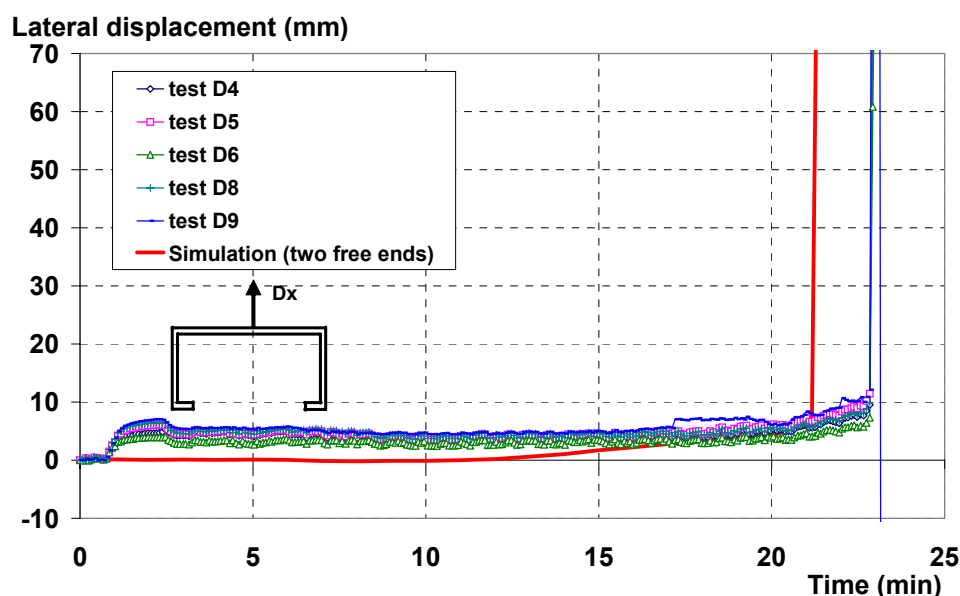


Figure 4-31: Comparison of lateral displacement of steel stud about weak axis between numerical simulation and fire test

Test	Stud	Length (mm)	Loading condition		Maximum test temperature (°C)	Calculated critical temperature (min)
			Load (kN)	Eccentricity (mm)		
Stud 1	medium	3500	15	37.5	257.0	467.0
Stud 2	medium	3500	25	0	245.0	230.0
Stud 3	medium	3500	15	0	500.0	541.0
Stud 4	large	3500	60	0	565.0	550.0
Stud 5	large	3500	60	0	540.0	550.0

Table 4-8: Comparison of failure temperature of studs engulfed in fire between numerical calculation and fire test

As a whole, the agreement between numerical modelling and tests can be considered as fully satisfactory and it is convenient to develop simple calculation model based on results obtained by means of numerical modelling.

#### 4.3.3.2 Numerical modelling of AWS-type cross section tall studs

The AWS section is a special section stud, so it is exclusively dealt within this paragraph. The basic geometry of the simulated AWS section is based on the nominal dimensions of the specimen tested at CTICM and is shown in Table 4-9 and Figure 4-32. Figure 4-33 shows two pictures of the modelled stud.

Length of the stud	3500 mm
Web height	20 + 110 + 20 mm
Flange width	40 + 50 mm
Edge fold	15.5 mm
Thickness used in numerical modelling (without zinc)	1.145 mm
Thickness (nominal)	1.2 mm

Table 4-9: Basic nominal geometry for the AWS section

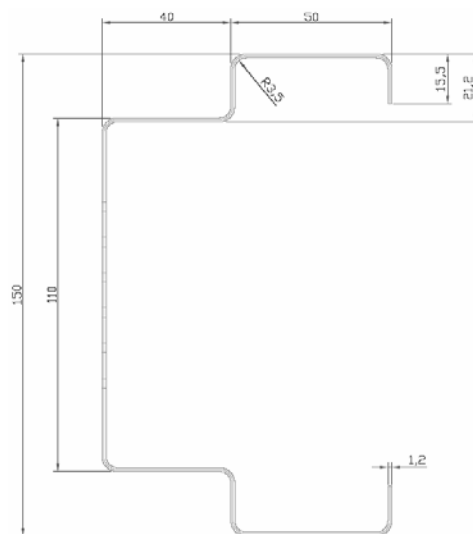


Figure 4-32: Basic nominal geometry of the tested AWS section

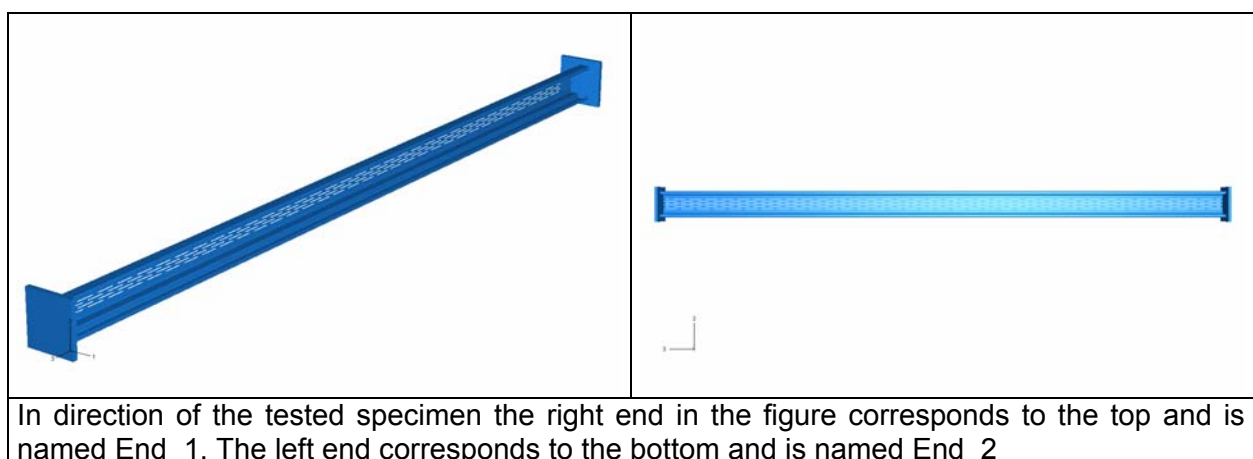


Figure 4-33: Modelled AWS steel stud

### **Numerical modelling of AWS-type section tall stud**

The model for AWS-type section tall stud consists of three different parts joined together to function as a whole structure. The different parts modelled are two endplates attached to the

ends of one section. The section was structurally modelled as one part and the endplates was structurally modelled as one part.

The steel stud was analysed with two different end boundary conditions. The displacement constraints and the rotational constraints used for the two different models are described in Table 4-10 and shown in Figure 4-34. Figure 4-36 shows the axis convention. Table 4-10 shows the degrees of freedom as they are referred to in Table 4-11.

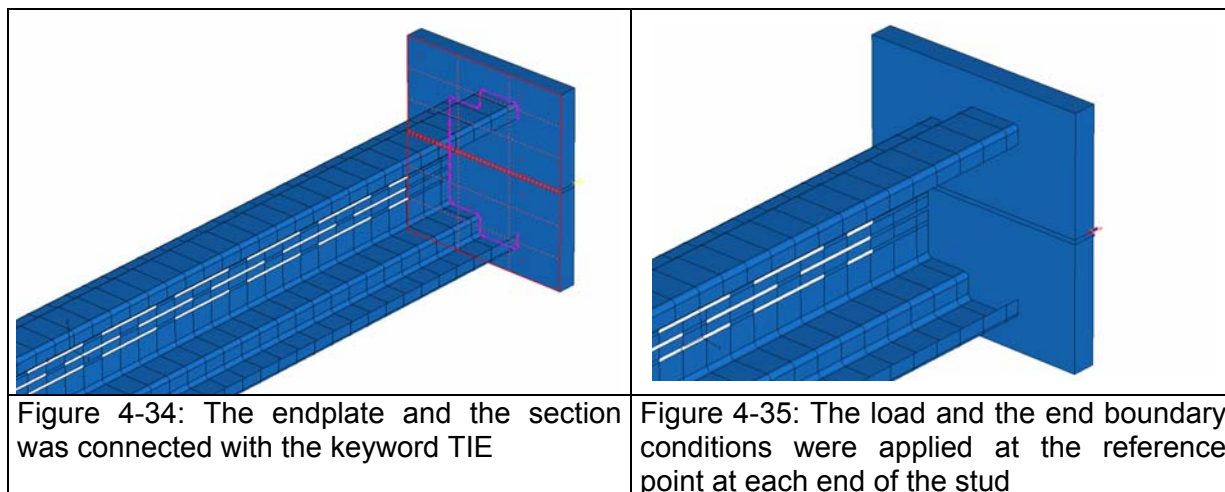
Convention	Degrees of freedom	Comment
U1	x-displacement	Displacement in direction 1
U2	y-displacement	Displacement in direction 2
U3	z-displacement	Displacement in direction 3
UR1	Rotation about the x-axis	Rotation about axis 1
UR2	Rotation about the y-axis	Rotation about axis 2
UR3	Rotation about the z-axis	Rotation about axis 3

Table 4-10: Symbols used for applying boundary conditions

Numerical model	Boundary condition at support – End_1	Boundary condition where the load is applied – End_2
FEA_1	U1=0, U2=0, U3=0 UR1=0, UR2=0, UR3=0	U1=0, U2=0 UR2=0, UR3=0
FEA_2	U1=0, U2=0, U3=0 UR2=0, UR3=0	U1=0, U2=0 UR2=0, UR3=0

Table 4-11: End boundary conditions for the different numerical models

The load was applied at the reference point at End\_2 (Figure 4-35). The load applied was similar to the load in the test (18 kN).



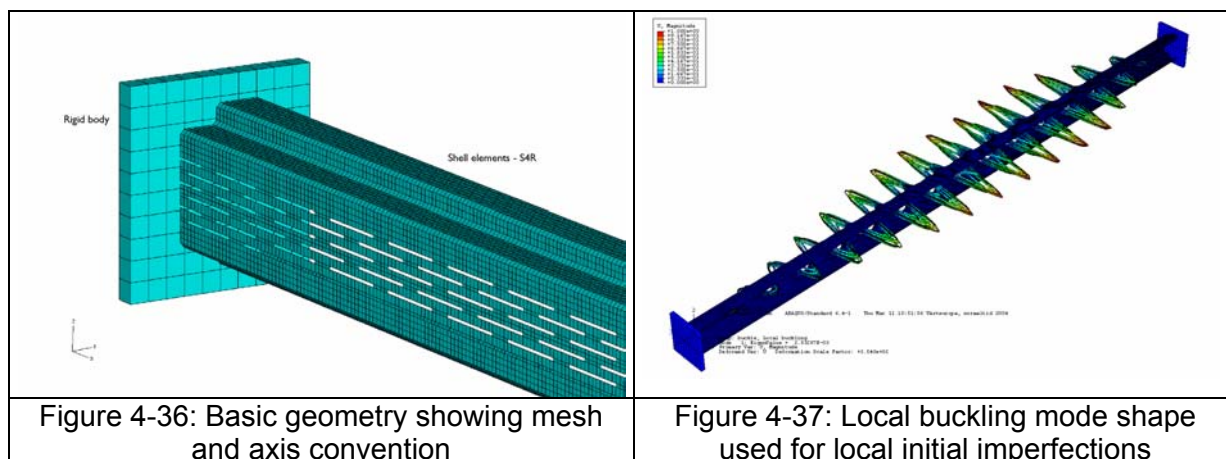
The steel section part was modelled with a 4-node shell element - S4R. The average element size was 6 mm. The end plates were modelled with rigid elements corresponding to a reference point where the load and boundary conditions was applied. The modelled steel stud was connected to the endplate using the keyword TIE in ABAQUS/Standard. This is suitable when joining parts together that may have different element types, mesh densities, etc. but the corresponding degrees of freedom at the boundary of each part can be equal.

To resemble the test conditions for the end of the steel stud and to apply the load into the steel stud correctly a 87 mm long part of the stud's ends where modelled using a thickness of 10 mm. The material properties for this part were taken with room temperature properties, but with a thermal expansion according to part 1.2 of Eurocode 3 [2].

Local imperfections were introduced by a perturbation in the geometry. In the numerical simulations the buckling mode shape was multiplied with a magnitude of  $b/200$ , where  $b$  is the width of the widest plate in the section. Global imperfection was introduced to the model by assuming an eccentric loading to the structure. The magnitude of the eccentricity was taken as  $L/1000$  (see Figure 4-36).

The yield strength and Young's modulus used in the numerical simulation were based on the data given in Chapter 2 (see Table 2-4). The material properties at elevated temperatures were calculated with the material model presented in part 1.2 of Eurocode 3 [2] with the yield strength and Young's modulus reduced at elevated temperatures with the proposed reduction factors proposed in Chapter 2 for **Type B** steel. The value of Young's modulus was taken as 210000 MPa. The coefficient of thermal expansion was taken according to 1.2 of Eurocode 3 [2] for all the elements except the rigid endplates.

The temperature evolution in the numerical model was applied at four different levels on the stud. The temperatures were taken as the mean value from different levels recorded in the test. The four different levels are illustrated in Figure 4-14. The mean value of the temperature was calculated from the five points A - E, at the layers N1, N2, N3 and N4, see Figure 4-38. The temperature curve used in the numerical simulations was also extended to a time beyond the failure time for the test. This has to be done because the temperature record from the test stops when failure of the steel stud occurs, in this case approximately after 29 minutes. From that point the temperature evolution was extended linearly to 55 minutes. The temperature variation across the section in the numerical simulation was neglected.



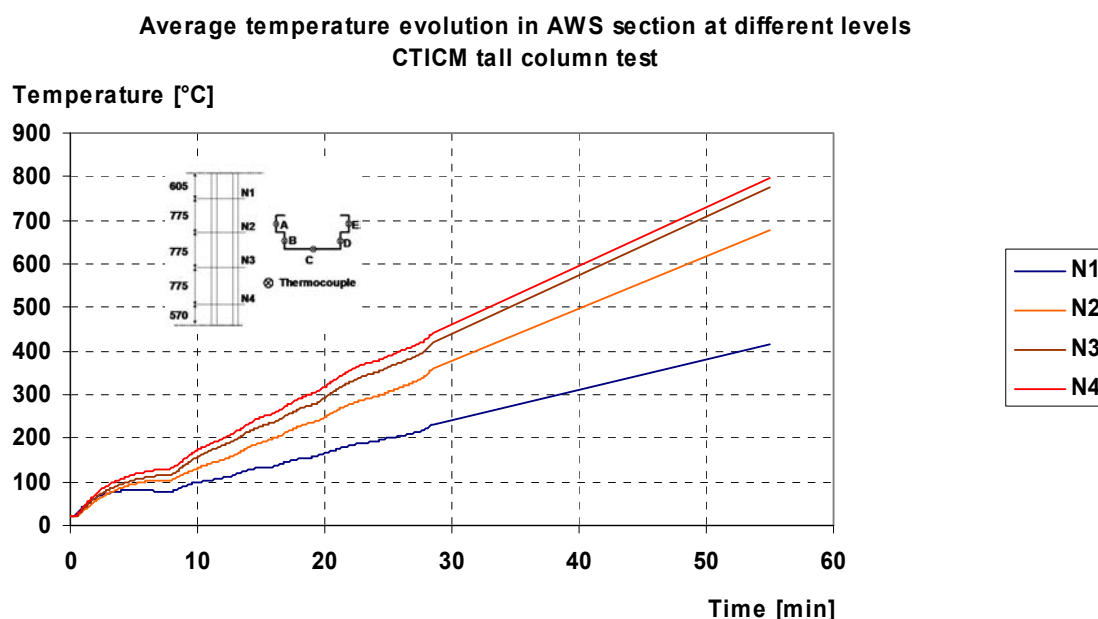


Figure 4-38: Temperature evolution at different levels used in the numerical simulation

### **Experimental results versus numerical simulations**

The result from the numerical simulations shows a good agreement with the test particularly the numerical model FEA\_1. The failure temperature recorded in the test is compared with the two simulations with different end boundary conditions in Table 4-12.

	Maximum failure temperature (°C) <sup>1</sup>	Numerical modelling/(CTICM test)
CTICM test	529	
FEA_1	501	0.95
FEA_2	479	0.91

Table 4-12: Summary of failure temperatures from test and numerical simulations

The displacements recorded in the numerical simulations are compared to the test and one example is shown in Figures 4-39 and 4-40. In some cases it can be difficult to compare the results because of the very small displacements. But it seems to correspond well with the test if the difference in the failure time is taken into account.

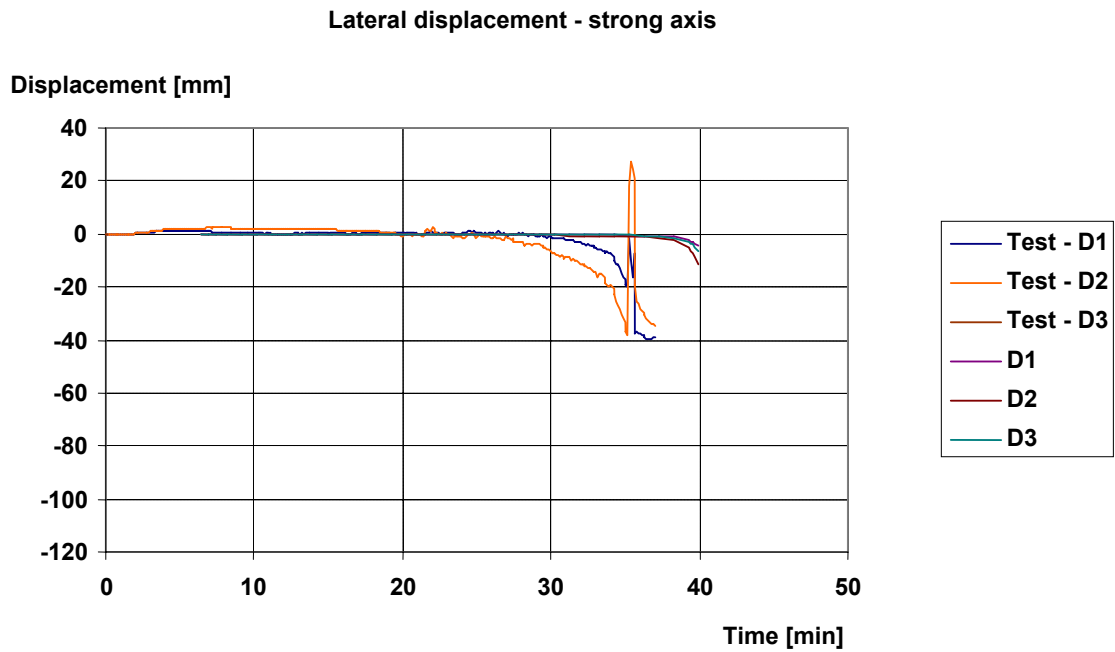


Figure 4-39: Lateral displacement along strong axis versus time for numerical model FEA\_1 compared to test results

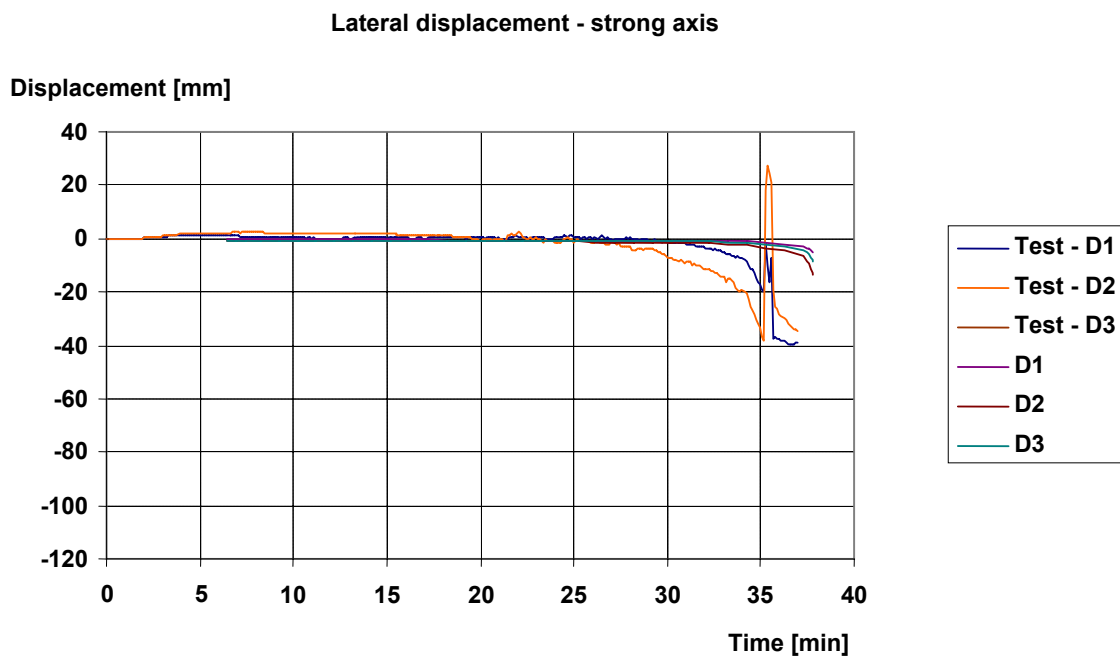


Figure 4-40: Lateral displacement along strong axis versus time for numerical model FEA\_2 compared to test results

## 4.4 DEVELOPMENT OF SIMPLE CALCULATION MODEL

### 4.4.1 General

The simple calculation model presented in this section gives a design proposal for isolated lightweight steel members and is proposed for two design situations:

- Uniform temperature distribution over the section,
- Non-uniform temperature distribution over the section with a thermal gradient taken into account by considering a thermal bow.

The temperature distribution along the stud is assumed to be uniform in both situations. The design model is based on expressions taking flexural buckling and lateral-torsional buckling into account in a way similar to that in part 1.3 of Eurocode 3 [1]. The load applied is an axial force that acts along the x-axis (length direction). The stud is assumed to rotate about the y-axis (strong axis) at supports. Different boundary conditions for rotation about the z-axis (weak axis) are considered.

In order to develop simple calculation rules, a parametric study was performed in which several parameters were studied. Based on the results of this parametric study the simple calculation model was evaluated. To avoid time-consuming calculations a simplified approach was taken as a starting point for the design method. First simplification is that all slenderness parameters  $\lambda$  for local and global buckling are calculated at 20°C. This simplification is based on the fact that  $f_{y,0.2,\theta} / E_{\theta}$  varies only slightly with temperature. It means that the reduction of the strength due to heating is solely taken into account by the use of  $f_{y,0.2,\theta}$  in the resistance formulae. Second simplification is that the bending due to the thermal gradient is considered equivalent to a constant bending moment. The reduction of the yield strength should be based on the temperature in the cross section as described below.

In the parametric calculations the steel stud was modelled with restrained rotation about weak axis at support, consequently no external bending moments about z-axis (weak axis) are applied. On the other hand, since the c-shaped section is mono symmetric about y-axis (strong axis) the possible shift of the centroid of the effective area  $A_{\text{eff}}$  relative to the gravity of the gross cross section gives an additional moment about z-axis (weak axis), which should be taken into account.

It is necessary to point out that the simple calculation model presented here is considered only to be valid for normal type c-section members.

### 4.4.2 Numerical parametric study with high studs engulfed in fire

For the purpose of developing simple calculation model for studs fully engulfed in fire, a parametric study was performed, in which following parameters have been studied:

- Length of steel stud: 600 mm, 3000 mm and 5100 mm
- Stud sections: 100x0.6, 150x1.2, 250x2.5
- Steel grade: S350 with  $f_y = 350$  MPa
- Temperature fields according to Figures 5-59 and 5-60: Uniform heating and heating with three different temperature gradients
- Boundary conditions: hinged about strong axis and restrained about weak axis
- Loading conditions: centric loading and eccentric loading  $0.5xh$  ( $h$  = web height of steel stud)

- Load levels:  $0.3 \times N_u$  and  $0.5 \times N_u$  ( $N_u$  according to numerical analysis at room temperature, refer to Table 4-13)

Loading condition	Length (mm)	Axial compression resistance $N_u$ (kN)		
		100x0.6	150x1.2	250x2.5
Centric loading	600	13.8	65.3	238.7
	3000	8.7	53.3	224.2
	5100	4.6	22.8	164.3
Eccentric loading	600	9.3	47.0	164.4
	3000	6.0	34.4	150.8
	5100	3.5	16.1	107.7

Table 4-13: Numerical compression resistance of steel studs at room temperature

A full parametric study was made at elevated temperatures according to the parameters explained. One example of the corresponding results is given respectively in figures 4-41 and 4-42 as well as in table 4-14 (for full results of this parametric study, refer to [30]).

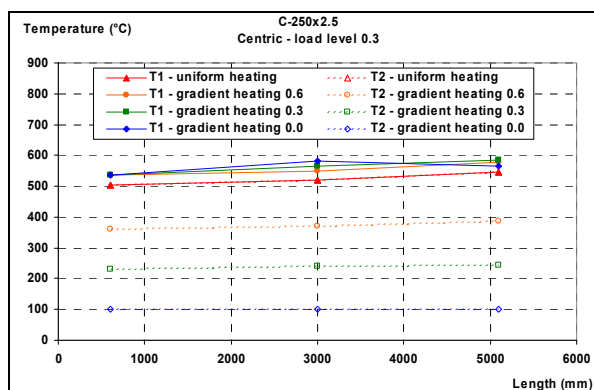


Figure 4-41: Critical temperature results of the numerical calculations (large section, centric load and load level of 0.3)

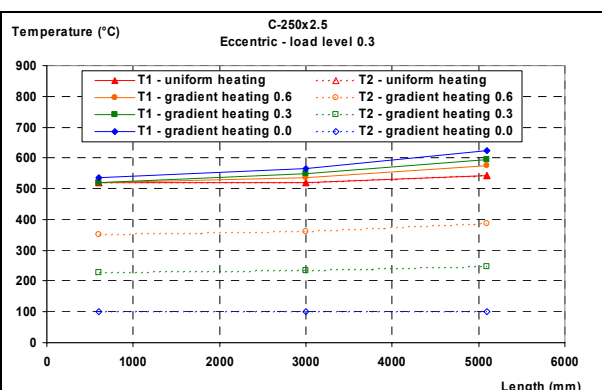


Figure 4-42: Critical temperature results of the numerical calculations (large section, eccentric load and load level of 0.3)

Load condition	Length (mm)	T1 = T2		T2 = 100+0.6x(T1-100)		T2 = 100+0.3x(T1-100)		T2 = 100	
		T1 (°C)	T2 (°C)	T1 (°C)	T2 (°C)	T1 (°C)	T2 (°C)	T1 (°C)	T2 (°C)
Centric load	600	505	505	535	361	535	231	535	100
	3000	520	520	550	370	565	240	580	100
	5100	546	546	578	387	584	245	565	100
Eccentric load on exposed side (0.5xh) <sup>(*)</sup>	600	520	520	520	352	520	226	535	100
	3000	520	520	535	361	550	235	565	100
	5100	543	543	577	386	595	249	625	100

(\*) h is the total depth of the cross section

Table 4-14: Critical temperatures for the C-250x2.5 section – load level of 0.3

It can be found from these results that:

- The critical temperature of steel studs, without any lateral supports, could have a critical temperature higher than 350°C which corresponds to the value of fixed critical temperature given in part 1.2 of Eurocode 3 [2] for all class 4 section steel elements.
- Temperature gradients do not lead to decreased critical temperatures of the studied elements (maximum temperature) even though the additional bowing effect could be very important. On the contrary, in some cases, the critical temperatures (maximum temperature) increase very slightly as temperature gradient increases

These results have been used in the development of simple calculation model presented hereafter.

#### 4.4.3 General principles of simple calculation model

The design includes a check of global buckling according to the applicable cases given in paragraphs 4.4.3.1 to 4.4.3.3 and a check of cross sectional resistance according to paragraph 4.4.3.4. Axis convention according to part 1.1 of Eurocode 3 was adopted.

##### 4.4.3.1 Buckling with uniform temperature distribution and centric load

The model of flexural buckling with centric load and uniform temperature distribution for an axially compressed steel stud is based on the equation given in part 1.3 of Eurocode 3 [1]. The equation is:

$$\frac{N_{fi,Ed}}{\chi_{\min} \cdot A_{eff} \cdot \frac{f_{y,\theta}}{\gamma_{M,fi}}} + \frac{N_{fi,Ed} \cdot e_N}{W_{eff,z} \cdot \frac{f_{y,\theta}}{\gamma_{M,fi}}} \leq 1 \quad (4-1)$$

$f_{y,\theta}$  is the 0,2 % proof strength at temperature  $\theta$  for the section according to relevant material model

$A_{eff}$  is the effective area of a cross section when subject to stresses due to uniform axial compression

$W_{eff}$  is the effective section modulus when subject only to bending stresses about relevant principal axis

The effective area  $A_{eff}$  and the effective section modulus  $W_{eff}$  should be determined in accordance to part 1.3 and 1.5 of Eurocode 3, i.e based on material properties at 20°C.

$N_{fi,Ed}$  is the design axial force in the fire design situation

$\gamma_{M,fi}$  is a partial safety factor for the fire design situation with recommended value 1.0

$e_N$  is the shift of the centroidal axis when the cross-section is subjected to uniform compression only

$\chi_{min}$  is the minimum of  $\chi_y$  and  $\chi_z$  and  $\chi_T$  (for normal C-sections  $\chi_z$  is smallest)

$\chi_T$  is the reduction factor due to torsional flexural buckling

$\chi_y, \chi_x$  is the reduction factor due to flexural buckling about relevant principal axis

$$\chi = \frac{1}{\phi + \sqrt{\phi^2 - \lambda^2}} \leq 1.0 \quad (4-2)$$

$$\lambda = \sqrt{\frac{f_{yb} A_{eff}}{N_{cr}}} \quad (4-3)$$

$$\phi = 0.5 \left[ 1 + \alpha (\lambda - 0.2) + \lambda^2 \right] \quad (4-4)$$

with  $\alpha = 0.34$  (buckling curve b)

$N_{cr}$  is the elastic critical force for the relevant buckling mode based on gross cross sectional properties at 20°C. Flexural buckling about relevant principal axis:

$$N_{cr} = \frac{\pi^2 EI}{l_c^2} \quad (4-5)$$

Torsional-flexural buckling:

$$N_{cr,TF} = \frac{N_{cr,y}}{2\beta} \left[ 1 + \frac{N_{cr,T}}{N_{cr,y}} - \sqrt{\left( 1 - \frac{N_{cr,T}}{N_{cr,y}} \right)^2 + 4 \left( \frac{y_0}{i_0} \right)^2 \frac{N_{cr,T}}{N_{cr,y}}} \right] \quad (4-6)$$

$$N_{cr,T} = \frac{1}{i_0^2} \left[ EK_w \frac{\pi^2}{l_c^2} + GK_v \right] \quad (4-7)$$

$$\beta = 1 - \left( \frac{y_0}{i_0} \right)^2 \quad (4-8)$$

$l_c$  is the relevant buckling length

$f_{yb}$  is the yield strength at 20°C of the base material

$y_0$  is the distance between shear centre and gravity centre along y-axis

$K_w$  is the warping constant of the gross cross section

$K_V$  is the torsion constant of the gross cross section  
 $E$  is Young's modulus at 20°C  
 $I$  is the second moment of area of the gross cross section about relevant principal axis

$$i_0^2 = \frac{I_y}{A_{gr}} + \frac{I_z}{A_{gr}} + y_0^2 \quad (4-9)$$

$A_{gr}$  is the gross cross sectional area

#### 4.4.3.2 Buckling with uniform temperature distribution and eccentric load

For members with mono-symmetric open cross sections (i.e. c-sections), account must be taken of the possibility that the resistance of the member to torsional-flexural buckling might be less than its resistance to flexural buckling. In case of eccentric loading and when the stud is laterally unrestrained the design check for torsional-flexural buckling is given by (4-10). In addition, (4-1) should be checked, which may govern for small moments  $M_y$ .

$$\left( \frac{N_{fi.Ed}}{\chi_{\min} \cdot A_{eff} \cdot \frac{f_{y,\theta}}{\gamma_{M,fi}}} \right)^{0.8} + \left( \frac{M_{y,fi.Ed}}{\chi_{LT} \cdot W_{eff,y} \cdot \frac{f_{y,\theta}}{\gamma_{M,fi}}} \right)^{0.8} \leq 1 \quad (4-10)$$

$f_{y,\theta}$  is the 0,2 % proof strength at temperature  $\theta$  according to relevant material model.

$M_{y,fi.Ed}$  is the bending moment about the y-axis (strong axis) in the fire design situation. If the load is applied eccentrically, then:

$$M_{y,fi.Ed} = N_{fi.Ed} \cdot e_z \quad (4-11)$$

$e_z$  is the eccentricity of the axial load

$$\chi_{LT} = \frac{1}{\phi_{LT} + \sqrt{\phi_{LT}^2 - \lambda_{LT}^2}} \leq 1.0 \quad (4-12)$$

$$\phi_{LT} = 0.5 \left[ 1 + \alpha (\lambda_{LT} - 0.2) + \lambda_{LT}^2 \right] \quad (4-13)$$

with  $\alpha = 0.21$

The non-dimensional slenderness due to torsional-flexural buckling can be written:

$$\lambda_{LT} = \sqrt{\frac{f_{yb} \cdot W_{el}}{M_{cr}}} \quad (4-14)$$

$W_{el}$  is the elastic section modulus of the gross cross section at 20°C

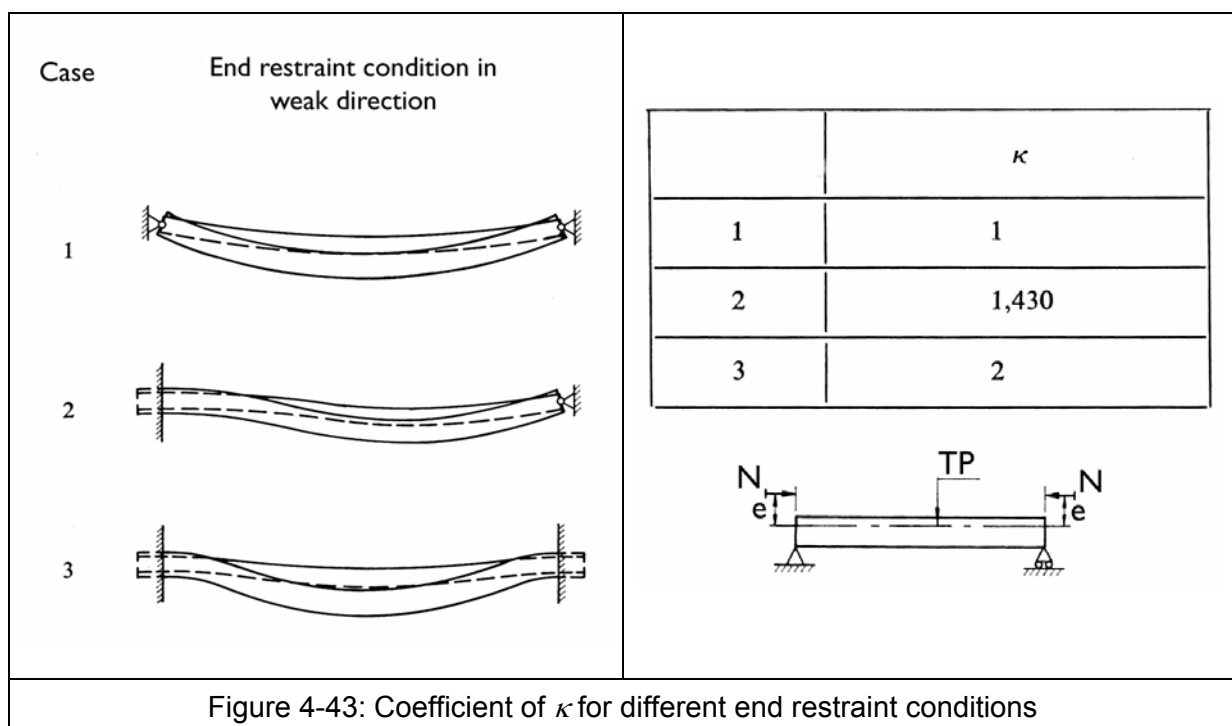
$M_{cr}$  is the elastic critical moment, which can be calculated according to:

$$M_{cr} = \frac{\kappa\pi}{L} \sqrt{EI_z \left( GK_v + \frac{\kappa^2 \pi^2 EK_w}{L^2} \right)} \quad (4-15)$$

$\kappa$  is a coefficient taken different end boundary conditions into account according to Figure 4-43, assuming same conditions for lateral bending and for warping.  
 $L$  is the length of the member

With  $K_v = 0$  equation (4-15) can be simplified to:

$$M_{cr} = \kappa^2 \pi^2 \frac{E \sqrt{I_z \cdot K_w}}{L^2} \quad (4-16)$$



#### 4.4.3.3 Flexural or torsional flexural buckling with temperature gradient

A thermal gradient causes a bow of the steel stud due to dissimilar thermal expansion of the flanges. The magnitude of the thermal deflection at midspan can be calculated from:

$$e_T = \frac{\alpha_T \cdot L^2 \cdot \Delta T}{8h} \quad (4-17)$$

$\alpha_T$  is the coefficient of thermal expansion,  $\alpha_T = 14 \cdot 10^{-6}$ .

$L$  is the length of the member

$\Delta T$  is the temperature difference between the colder flange and the warmer flange

$h$  is the web height

The bow causes an eccentricity in the z-direction (weak axis), which has to be added to the bending moment caused by eccentric axial load. The two cases considered is first when the

bending moment due to eccentric load on the warm side decreases the thermal bowing, and second when the eccentric load is applied on the cold side which increases the thermal bowing. Note that the thermal eccentricity can be larger than the eccentricity of the load. Thus the design check for the first case can be written:

$$\left( \frac{N_{fi.Ed}}{\chi_{\min} \cdot A_{eff} \cdot \frac{f_{y,\theta,max}}{\gamma_{M,fi}}} \right)^{0.8} + \left( \frac{N_{fi.Ed} \cdot |(e_z - e_T)|}{\chi_{LT} \cdot W_{eff,y} \cdot \frac{f_{y,\theta,max}}{\gamma_{M,fi}}} \right)^{0.8} \leq 1 \quad (4-18)$$

$f_{y,\theta,max}$  is the 0,2 % proof strength at temperature  $\theta$  for the hot flange according to relevant material model.

Similarly for the second case:

$$\left( \frac{N_{fi.Ed}}{\chi_{\min} \cdot A_{eff} \cdot \frac{f_{y,\theta,av}}{\gamma_{M,fi}}} \right)^{0.8} + \left( \frac{N_{fi.Ed} \cdot (e_z + e_T)}{\chi_{LT} \cdot W_{eff,y} \cdot \frac{f_{y,\theta,av}}{\gamma_{M,fi}}} \right)^{0.8} \leq 1 \quad (4-19)$$

$f_{y,\theta,av}$  is the 0,2 % proof strength at temperature  $\theta$  for the average temperature over the section according to relevant material model.

#### 4.4.3.4 Cross sectional resistance

In addition to the check for global buckling, a check of the cross sectional resistance should be done. This may govern for short studs.

Centric load with uniform temperature distribution:

$$\frac{N_{fi.Ed}}{A_{eff} \cdot \frac{f_{y,\theta}}{\gamma_{M,fi}}} + \frac{N_{fi.Ed} \cdot e_N}{W_{eff,z} \cdot \frac{f_{y,\theta}}{\gamma_{M,fi}}} \leq 1 \quad (4-20)$$

Eccentric load with uniform temperature distribution:

$$\frac{N_{fi.Ed}}{A_{eff} \cdot \frac{f_{y,\theta}}{\gamma_{M,fi}}} + \frac{M_{y,fi.Ed}}{W_{eff,y} \cdot \frac{f_{y,\theta}}{\gamma_{M,fi}}} + \frac{N_{fi.Ed} \cdot e_N}{W_{eff,z} \cdot \frac{f_{y,\theta}}{\gamma_{M,fi}}} \leq 1 \quad (4-21)$$

Centric load with temperature gradient:

$$\frac{N_{fi.Ed}}{A_{eff} \cdot \frac{f_{y,\theta,max}}{\gamma_{M,fi}}} + \frac{N_{fi.Ed} \cdot e_T}{W_{eff,y} \cdot \frac{f_{y,\theta,max}}{\gamma_{M,fi}}} + \frac{N_{fi.Ed} \cdot e_N}{W_{eff,z} \cdot \frac{f_{y,\theta,max}}{\gamma_{M,fi}}} \leq 1 \quad (4-22)$$

Eccentric load on the warm side with temperature gradient:

$$\frac{N_{fi.Ed}}{A_{eff} \cdot \frac{f_{y,\theta,max}}{\gamma_{M,fi}}} + \frac{N_{fi.Ed} \cdot |(e_z - e_T)|}{W_{eff,y} \cdot \frac{f_{y,\theta,max}}{\gamma_{M,fi}}} + \frac{N_{fi.Ed} \cdot e_N}{W_{eff,z} \cdot \frac{f_{y,\theta,max}}{\gamma_{M,fi}}} \leq 1 \quad (4-23)$$

Eccentric load on the cold side with temperature gradient:

$$\frac{N_{fi.Ed}}{A_{eff} \cdot \frac{f_{y,\theta,av}}{\gamma_{M,fi}}} + \frac{N_{fi.Ed} \cdot (e_z + e_T)}{W_{eff,y} \cdot \frac{f_{y,\theta,av}}{\gamma_{M,fi}}} + \frac{N_{fi.Ed} \cdot e_N}{W_{eff,z} \cdot \frac{f_{y,\theta,av}}{\gamma_{M,fi}}} \leq 1 \quad (4-24)$$

#### 4.4.4 Comparison of mechanical performance of studs engulfed in fire between simple calculation model and advanced numerical model

In order to show the validity of proposed simple calculation model described in previous paragraph, results of numerical calculations are compared to simple calculation method (see example for the medium section in Tables 4-15 and 4-16). It can be found that the agreement is quite well. It is worth mentioning that ratio  $b/t$  for the small section is 83, which is larger than 60. It means that this cross section is outside the range of validity of procedure given in part 1.3 of Eurocode 3.

$T_{cr}$	$N_{FEA}$	$N_{u.code}$	$T_{cr}$	$N_{FEA}$	$N_{u.code}$	$T_{cr}$	$N_{FEA}$	$N_{u.code}$
520	14.1	11.4	535	10.3	8.1	579	4.8	3.6
400	23.5	18.8	416	17.2	13.6	482	8.0	5.9

Table 4-15: Comparison between simple calculation method and numerical calculations for medium section (Uniform temperature, eccentric loading)

$T_{cr}$	$N_{FEA}$	$N_{u.code}$	$T_{cr}$	$N_{FEA}$	$N_{u.code}$	$T_{cr}$	$N_{FEA}$	$N_{u.code}$
520	19.6	18.4	535	16	14.5	579	6.9	7.9
400	32.7	30.6	416	26.6	25.5	482	11.4	13.2

Table 4-16: Comparison between simple calculation method and numerical calculations for medium section (Uniform temperature, centric loading)

In addition, in Figures 4-44 to 4-45 is given the comparison between results of the numerical calculations and the simplified calculation method for studs submitted to centric and eccentric axial load, with uniform temperature over the section for the small, medium and large section respectively.

From these figures, it can be found that:

- For centric and eccentric loading with uniform temperature over the section, the simplified method can predict the buckling resistance very well compared to the numerical calculations. As seen from Figure 4-44 and 4-45 all points can be found on the safe side.

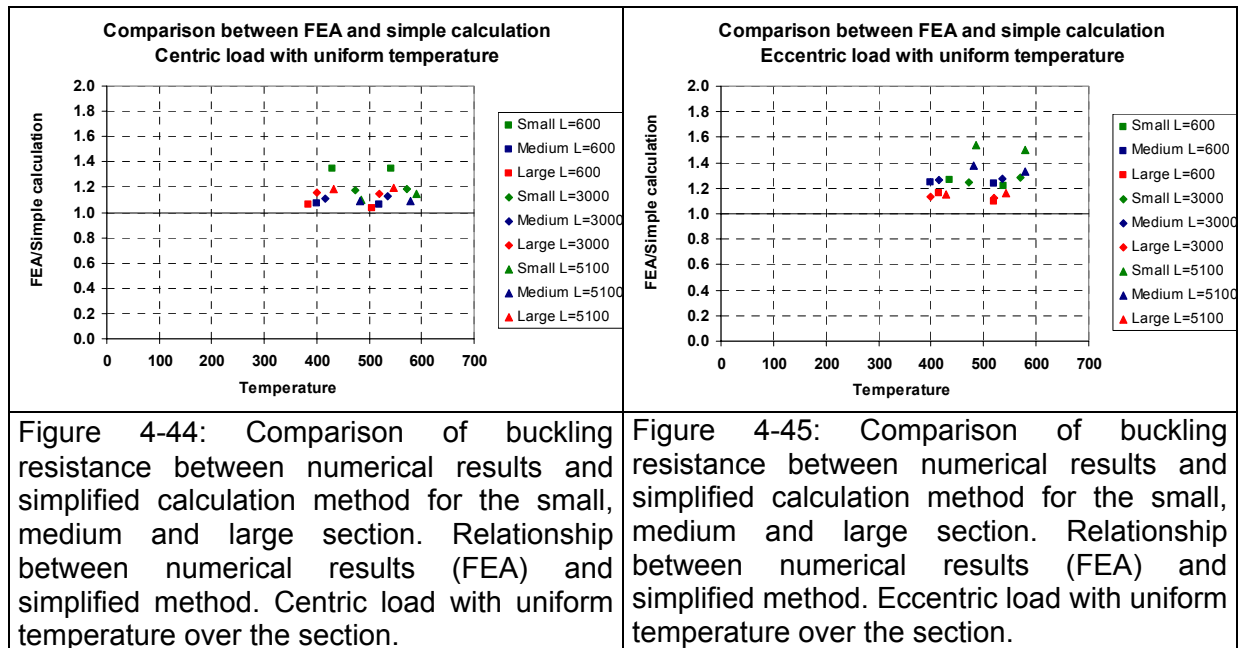
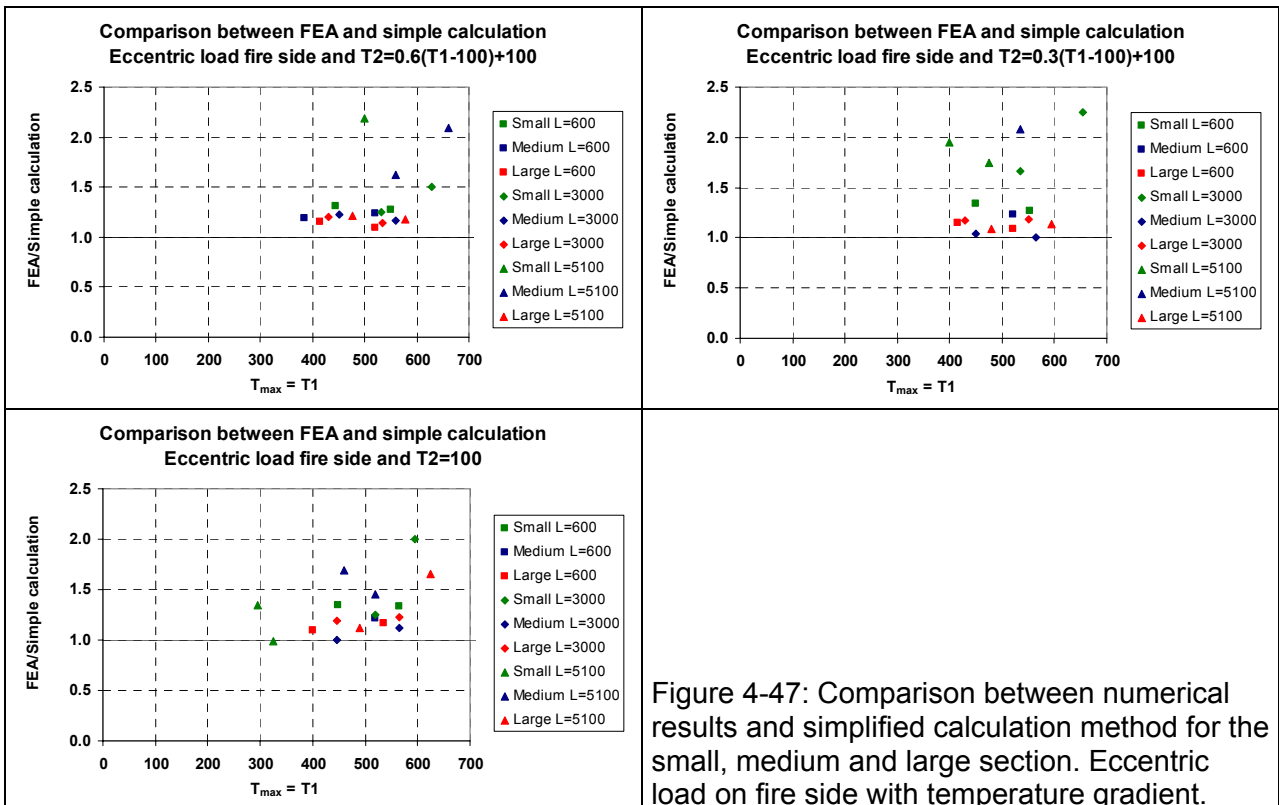
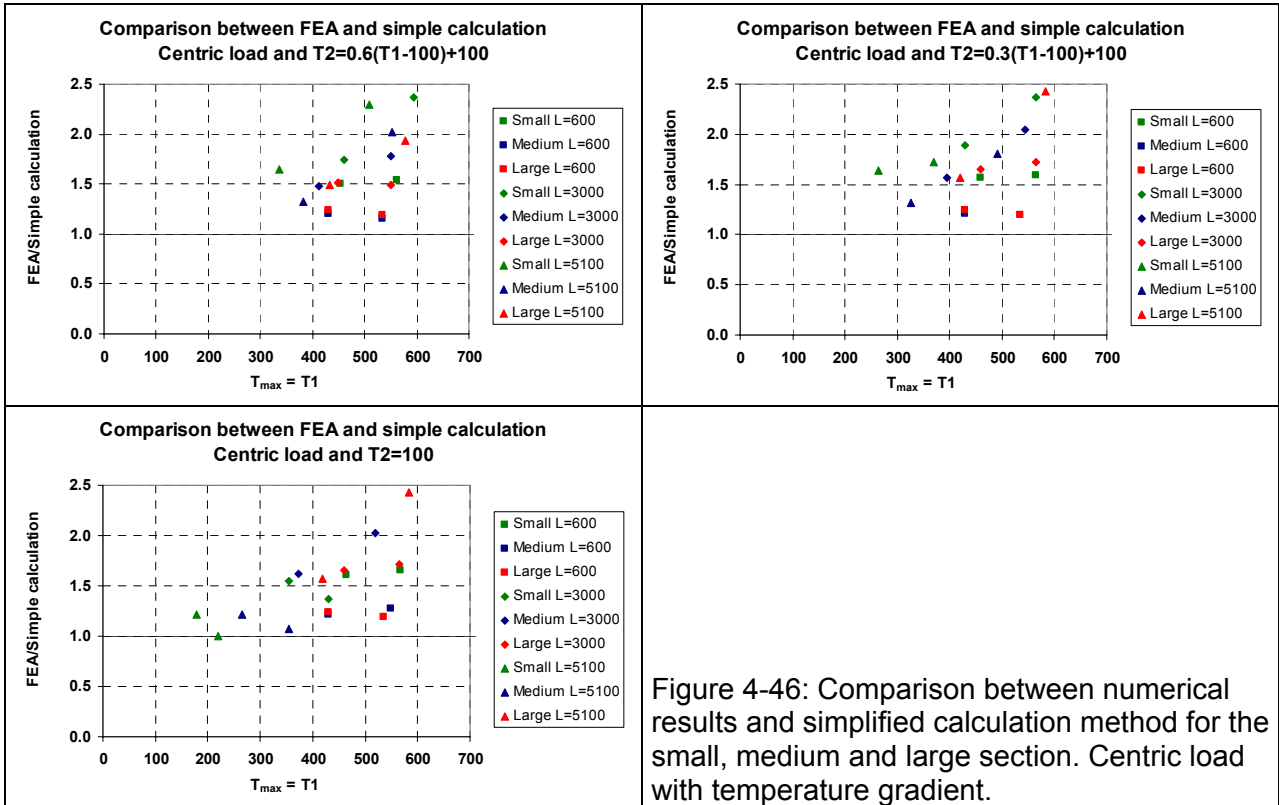
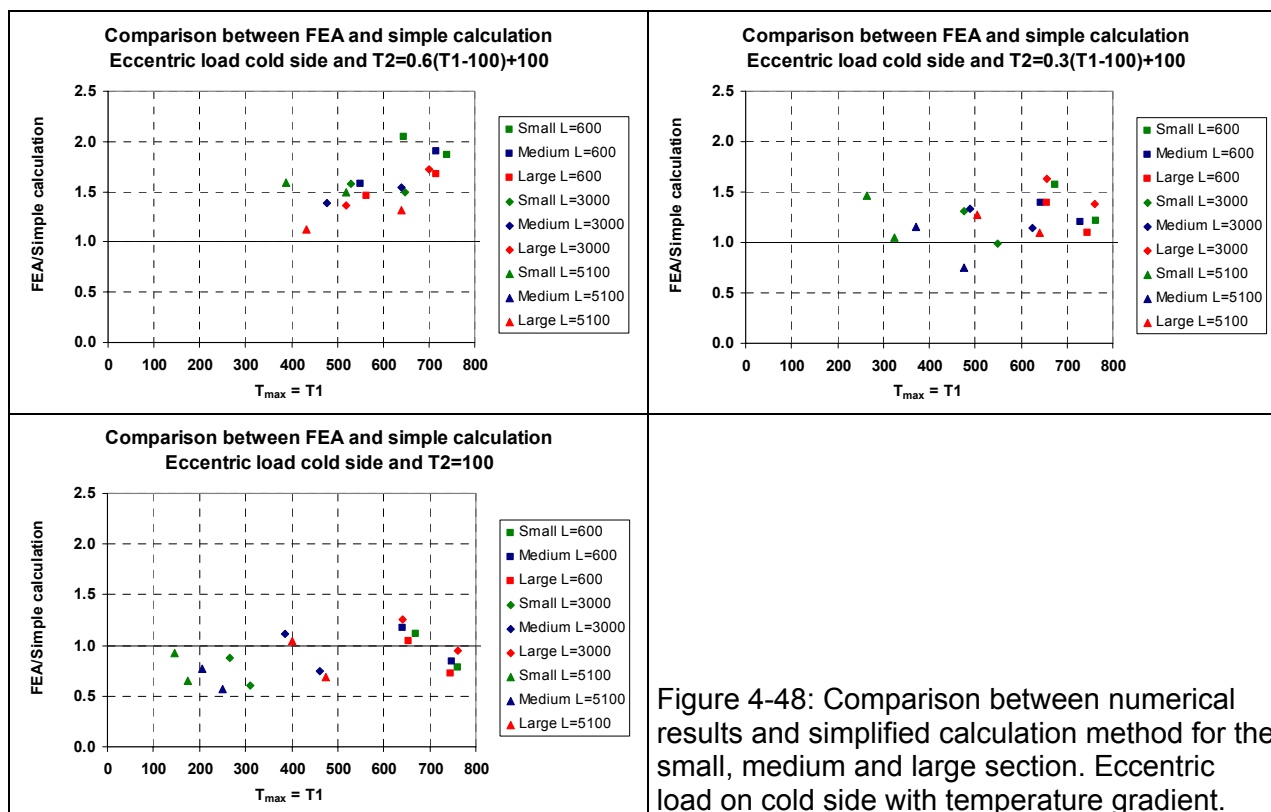


Figure 4-46 to 4-48 shows the comparison between results of the numerical calculations and the simplified calculation method for studs submitted to centric and eccentric load, with temperature gradient over the section for the small, medium and large section respectively. A temperature gradient over the section is not in reality reasonable when the stud is fully engulfed in fire, but it is necessary to be able to predict the mechanical behaviour when subjected to temperature differences to increase the understanding of failure mechanisms of lightweight steel section in fire. From these figures, it can be found that:

- The results show rather big scattering when a temperature gradient over the section is considered. However, the results are always on the safe side except when considering large temperature gradients and eccentric loading on the cold side.
- As seen from Figure 4-47, when the load is applied eccentrically on the fire side, the scattering decreases slightly. This could be explained by the fact that the reduction factor is used for the hot flange where the load is applied.





## 4.5 CONCLUSIONS

Lightweight steel members are often class 4 section elements, so they are very sensitive to local buckling behaviour. For that reason it is important to know what the appropriate characteristic values should be to be used in design in order to assess the mechanical resistance in the right way. As a consequence, one part of the work presented in this chapter was focused on this aspect. First of all, the stub column tests have been carried out on three different C-type sections and one special section called as AWS, which has helped to get an experimental basis for validating the numerical modelling. Secondly, the application of numerical modelling to different stub columns shows that under fire situation, the 0.2 % proof characteristic strength rather than 2% effective strength should be used to predict the local buckling resistance of lightweight steel members since the reduction strength of stub columns follows closely the reduction factor in respect to this characteristic strength. In addition, the reduction factors given in part 1.2 of Eurocode 3 [2] could lead to unsafe assessment for lightweight steel members under fire situation and the proposal of Chapter 2 for **Type B** steel can be considered as appropriate values to be used instead.

Also in some cases, load-bearing lightweight steel members could be fully engulfed in fire. Their mechanical performance needs to be predicted. Nevertheless, there is no design rule for fire situation regarding this feature. Consequently, another part of the work within the scope of this chapter is related exclusively to the behaviour of high studs in lightweight steel surrounded entirely by fire. Several tests have been performed on high studs with different cross sections. The numerical modelling is also validated against these tests and then applied in a parametric study. Based on the results of above study, a simple calculation model available for C-type section members is proposed. The comparison of this simple design rule with parametric study show a good agreement for uniformly heated members, which in fact correspond the most common situation of lightweight steel studs engulfed in

fire. Nevertheless, if temperature gradient exists on cross section of isolated lightweight steel studs, the simple calculation model predicts quite different results from numerical analysis. This phenomenon is very possibly due to the fact that the section is no longer a homogeneous section in stiffness and strength leading to a very different torsional behaviour and as a consequence an important scatter between numerical analysis and simple calculation model based on homogeneous sectional properties.

## Referenser som rapporten hänvisar till

- [1] CEN "General rules, Supplementary rules for cold-formed thin gauge members and sheeting", English version of part 1.3 of Eurocode 3, 27th September 2002
- [2] CEN "Design of steel structures, general rules, Structural fire design", part 1.2 of Eurocode 3, 27th April 2003
- [3] J. Outinen "Transient state tensile results of structural steels S235, S355 and S350GD+Z at elevated temperatures", Helsinki University of Technology, 1995
- [4] ECSC "Development of the use of stainless steel in construction (contract 7210-SA/842)", work package 5.1 of final report, 1999
- [5] CTICM "Calculation Rules of Lightweight Steel Sections in Fire Situation", Appendix A of Second annual technical report, 27th March 2001
- [6] CTICM "Calculation Rules of Lightweight Steel Sections in Fire Situation", Appendix A of Second semester technical report, 24th September 2001
- [7] CEN "General rules, Rules for buildings", English version of part 1.1 of Eurocode 3, 27th September 2002
- [8] Alfawakhiri, F. and Sultan, M.A. "Fire Resistance of Load-Bearing Steel-Stud Walls Protected with Gypsum Board", Proc. Fire and Materials '99, Interscience Communications Ltd., San Antonio, TX, USA, 1:235-246, 1999
- [9] CTICM "Fire resistance of a tall distributive partition wall of type PREGYMETAL D106/70 – 50/40A", Test report, 17th of March 1999
- [10] CTICM "Fire Resistance of an assembly consisted of a partition and a floor, each of them made of steel frameworks and plasterboard facings", Test report 03-U-163, 30<sup>th</sup> April 2003
- [11] CTICM "Fire Resistance of an assembly consisted of a partition and a floor, each of them made of steel frameworks and plasterboard facings", Test report 03-U-334, 2<sup>nd</sup> October 2003
- [12] CTICM "Fire Resistance of an assembly consisted of a partition and a floor, each of them made of steel frameworks and plasterboard facings", Test report 03-U-392, 12<sup>th</sup> November 2003
- [13] PR 254 N 83 "Test report on fire tests of lightweight steel sections maintained by plasterboards", VTT
- [14] Fire test of building elements "Test report 02-U-007", CTICM
- [15] PR 254 N 92 - Appendix D "Summary of fire test results with steel studs maintained by plasterboards", CTICM
- [16] PR 254 N 72 Appendix G "Calculation rules of lightweight steel sections in fire situation, validation study of mechanical behaviour of steel stud maintained by board, ANSYS results", CTICM, B. ZHAO
- [17] PR 254 N 72 Appendix H "Calculation rules of lightweight steel sections in fire situation, Numerical analysis of a steel stud at room and under elevated temperatures with the software SAFIR", ProfilARBED
- [18] PR 254 N 87-C "Validation study of the mechanical behaviour of a steel stud - ABAQUS results ", VTT, Olli Kaitila
- [19] PR 254 N 72 Appendix F "Calculation rules of lightweight steel sections in fire situation", LABEIN
- [20] PR 254 N 93-A "Lightweight steel sections maintained by boards at elevated temperature: Numerical simulation of fire tests", CTICM, C. RENAUD
- [21] PR 254 N 95-A "Lightweight steel sections maintained by boards at elevated temperature: Numerical simulation of two fire tests", CTICM, C. RENAUD

- [22] PR 254 N 122-A "Numerical simulations of VTT fire Tests 13, 14 and 15 on C250-80-21.5/2.5 - steel sections maintained by plasterboards", VTT, Olli Kaitila
- [23] PR 254 N 107-A "Numerical simulations of VTT fire Tests 3, 5 and 18 and CTICM fire tests 2 and 5 on lightweight steel sections maintained by boards", VTT, Olli Kaitila
- [24] [24] PR 254 N 108-A "Numerical simulations of VTT fire Tests 10, 11 and 12 on AWS -steel sections maintained by plasterboards", VTT, Olli Kaitila
- [25] PR 254 N 88-C «Parametric study of studs maintained by boards", CTICM, C. RENAUD
- [26] PR 254 N 109-A "Parametric study of AWS sections maintained by boards in fire", VTT, Olli Kaitila
- [27] PR 254 N 113-A "Comparison between simple calculation rule and ANSYS results ", CTICM, C. RENAUD
- [28] French methodology for extended application of partition test results for tall partitions INC-02/147-JK/IM
- [29] Group of notified bodies-Fire Sector Group - Rules for extended application of fire resisting elements FSG N162
- [30] CTICM "Calculation Rules of Lightweight Steel Sections in Fire Situation", Appendix K of Fourth annual technical report, 30th March 2004
- [31] VTT "Mechanical Behaviour of Lightweight Steel Sections at Elevated Temperatures", test report, 29th November 2002
- [32] CTICM "Mechanical Resistance of 3 Types of Cold Rolled Studs for lightweight Partitions under Slow Heating Conditions", test report, 29th March 2004